



# Hidden Heat: The case of 2023 Gulf of Trieste Bottom Marine Heatwave

Fabio Giordano<sup>1,\*</sup>, Matjaž Ličer<sup>2,3</sup>, Stefano Querin<sup>1</sup>, Stefano Salon<sup>1</sup>, and Martin Vodopivec<sup>2,\*</sup>

<sup>1</sup>National Institute of Oceanography and Applied Geophysics - OGS, Italy

<sup>2</sup>National Institute of Biology, Marine Biology Station Piran, Slovenia

<sup>3</sup>Slovenian Environment Agency, Slovenia

\*These authors contributed equally to this work.

**Correspondence:** Martin Vodopivec (martin.vodopivec@nib.si)

**Abstract.** In summer and autumn 2023, unusually high bottom temperatures were recorded at the Vida buoy (LTER site, 22 m depth) in the Gulf of Trieste (northern Adriatic, Mediterranean Sea). This long-term dataset enabled rare in situ observation of a bottom marine heatwave (BMHW), which began in early August and lasted over three months. At its peak, bottom temperature reached 4.3°C above the 20-year average and 1.2°C above the previous maximum recorded since 2002. Observations and  
5 modelling indicate that the BMHW was preconditioned by a prolonged drought starting in 2022 and continuing into 2023. This resulted in elevated surface salinity and weakened stratification, allowing unusually deep mixing that extended to the seafloor. Although 2023 was warm, heat was distributed over a thicker water column than usual, limiting sea surface warming but causing  
10 extreme temperatures at depth. The event persisted into autumn due to freshwater inflow, which re-established stratification and trapped the heat below. As surface temperatures remained moderate, the BMHW was undetectable by satellites or surface measurements. Only bottom sensors and models revealed the stress in deeper layers. Such events may therefore remain unnoticed while exerting extreme stress on the marine ecosystem. Our findings highlight reduced precipitation and deep mixing as overlooked drivers of subsurface marine heatwaves, which may become more frequent in similar shallow and stratified areas subject to increasingly frequent droughts driven by climate change.



## 1 introduction

15 Climate change is increasing environmental risks on most ecosystems through numerous pathways. Persistent warming trends in the global oceans, reaching from the ocean surface (von Schuckmann et al., 2024; Plecha and Soares, 2020) to bathypelagic depths, lead to an increase in thermal and other stressors for pelagic and benthic organisms (Boyd et al., 2015). One of the most frequent short timescale harbingers of these long-term processes are periods of prolonged anomalously warm ocean temperatures with far reaching consequences for coastal communities and marine ecosystems (Estournel et al., 2025; Brown et al., 2021; Garrabou et al., 2022). These anomalies are most often referred to with a generic broad term of marine heatwaves (MHWs), and lead to a series of dramatic undesired effects in the ocean, from mass mortality events to shifts in ecosystemic community structures (Garrabou et al., 2022; Gómez-Gras et al., 2021; Gómez-Gras et al., 2021), but can also impact dominant climate modes (Holbrook et al., 2019) and contribute to compound extreme events (Rodrigues et al., 2025; Gruber et al., 2021), such as atmospheric heatwaves and heavy precipitation events, boosting risks of regional flooding and coastal region wildfires. 25 They are typically defined as prolonged periods of anomalously warm ocean temperatures relative to the local climate baseline (often above the 90th percentile for the respective day of year) lasting at least 5 days (Hobday et al., 2016). Both thresholds for this MHW definition, the percentiles and the 5-day period, are somewhat arbitrary, however they will be used in this study as well to stay in line with previous works on the topic.

Bottom marine heatwaves (BMHW) are an analogous phenomenon occurring near the ocean floor and can be identified along similar lines. For example, Amaya et al. (2023a) classify a month as experiencing a BMHW if the detrended bottom temperature anomaly exceeds the 90th percentile for that calendar month, analogous to surface MHW detection. BMHWs arise from an interplay of oceanic processes and atmosphere-ocean interactions (Malan et al., 2025). In comparison to surface events, which can be studied on the basis of satellite observations, BMHWs are less well understood due to lack of deep sea and benthic temperature measurements. Their intensity and longevity can however exceed that of a surface MHW (Capotondi et al., 2024; Darmaraki et al., 2019). Furthermore, extremely intense BMHWs without any surface indication are not uncommon (Amaya et al., 2023a). For example, during a given marine heatwave event, the seafloor in some regions can be warmer relative to its baseline than the surface layer is relative to its respective baseline. 35

Open ocean surface MHWs are often driven by intense atmosphere-ocean heat fluxes, accumulating heat above the thermocline (Denaxa et al., 2024). This mechanism however typically doesn't explain deep and bottom marine heatwaves. BMHWs are typically driven by atmospheric heating of the stratified surface layer due to the presence of an atmospheric heatwave (Pastor and Khodayar, 2023), followed by a period of stratification weakening, water column mixing and warm water entrainment. This way a surface MHW can be translated into a bottom MHW. Another option for a BMHW generation is horizontal warm water advection in the deep layer, raising temperature close to the seafloor and lacking a significant surface signature. An existing weak stratification may be a relevant preconditioning factor which controls whether a BMHW can occur and how long it will last. Since they are not losing heat to the atmosphere, BMHWs can be very persistent (Amaya et al., 2023a). Salinity's role is twofold: it influences stratification strength and can indicate water mass changes. A fresher surface will strengthen stratification and trap the heat in the surface layer above the pycnocline. This can intensify the surface MHW intensity while shielding the 45



bottom from immediate warming. In contrast, weak salinity stratification allows for easier vertical mixing. Therefore, salinity profiles can either amplify or dampen a heatwave's vertical reach.

50 Previous research on the biological effects of MHWs has shown that the most devastating mass mortality events occur in benthic communities (Konsta et al., 2026; Estournel et al., 2025; Garrabou et al., 2022; Smale et al., 2019; Garrabou et al., 2009). Whereas pelagic species can often seek refuge in deeper, colder waters (Smith et al., 2023), benthic species are not mobile and therefore cannot escape overheating (Smale et al., 2019; Galli et al., 2017). Benthic organisms are also threatened by BMHWs, which by definition occur at the bottom and sometimes without a surface signal. The Mediterranean Sea is a  
55 known biodiversity hotspot vulnerable to climate change (Konsta et al., 2026; Simon et al., 2022; Tuel and Eltahir, 2020), and ocean warming has already affected Mediterranean biota (Azzurro et al., 2019), including in the Adriatic Sea and its northernmost part—the Gulf of Trieste (Figure 1) (Donša et al., 2026; Gianni et al., 2025; Glamuzina et al., 2024; Bevilacqua et al., 2019). A historical overview of invertebrate mass mortality events in the Mediterranean Sea between 1945 and 2011 showed that these coincided with positive temperature anomalies (Rivetti et al., 2014). A study of more recent (2015–2019)  
60 Mediterranean mass mortality events identified Cnidaria, Bryozoa, and Rhodophyta as the most affected taxonomic groups (Garrabou et al., 2022), while a study on future BMHWs in the Mediterranean Sea indicates that benthic Cnidaria, Crustacea, and Echinodermata will experience the most thermal stress in the coming decades (Konsta et al., 2026). However, the effects of BMHWs are not limited to benthic species and have been linked to reduced cod recruitment and redistribution of some fish species (Amaya et al., 2023a; Fogarty et al., 2008). Interestingly, Garrabou et al. (2022) identified depths between 15 m and 20  
65 m as the most deadly, and a large proportion of our study area (the Gulf of Trieste, Figure 1) lies within this depth range.

In this paper we present one of the first in situ observations of a BMHW complemented by high resolution ocean model simulations. A long term dataset including bottom temperatures, combined with surface salinity, temperature and other environmental variables, enabled us to establish a solid baseline and thoroughly analyze the event, its dynamics and environmental factors that caused it. A high resolution numerical simulation provided a full three-dimensional view and temporal evolution  
70 of the event.



## 2 Methods

### 2.1 Study area

The impact of marine heatwaves is closely linked to the general climatic and oceanographic context of the region in which they occur. The Mediterranean Sea is a well-known hot spot for marine heatwaves and climate change (Pastor et al., 2024; Hamdeno and Alvera-Azcaráte, 2023; Cos et al., 2022). At the basin scale, a negative freshwater budget—where evaporation exceeds precipitation and runoff—is compensated by a surface inflow of Atlantic Water through the Strait of Gibraltar. This circulation contributes to the formation of a relatively well-defined pycnocline in the Western Mediterranean, which enhances the basin's susceptibility to marine heatwaves (Simon et al., 2022).

The Adriatic Sea forms the northern part of the central Mediterranean and represents a dilution basin (Gačić et al., 2001), receiving freshwater input from more than forty rivers. Approximately one third of the total Mediterranean river discharge enters through the Adriatic basin (Boicourt et al., 2020). The combination of freshwater input and atmospheric forcing results in a marked seasonal cycle, with pronounced stratification during summer under calm conditions, and a well-mixed water column during autumn and winter driven by strong NE and SE winds.

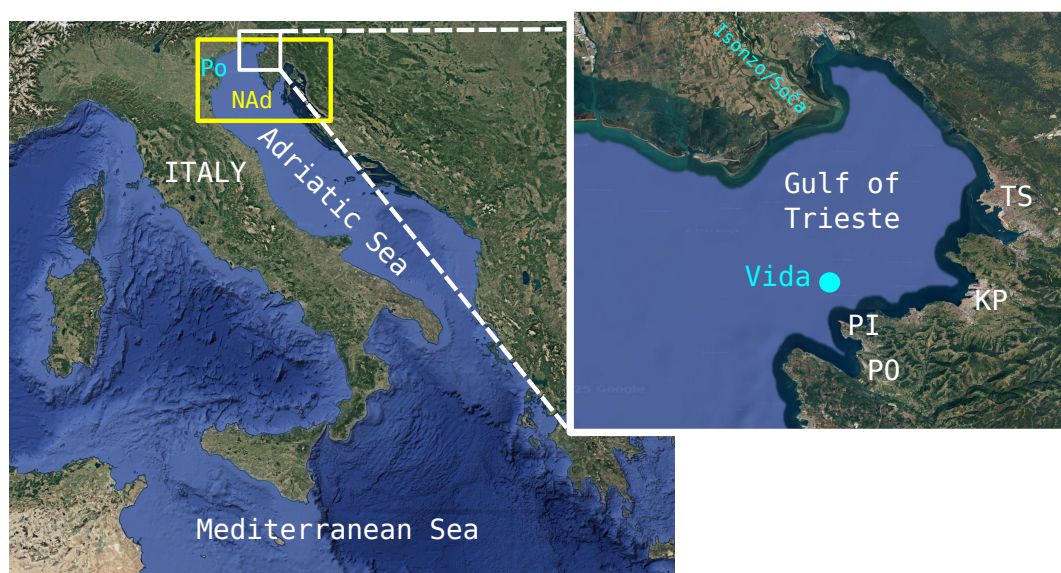


**Figure 1.** Study area (background map from © Google Earth). Yellow rectangle denotes Northern Adriatic (NAd) MITgcm modeling domain. White rectangle and inset on the right show the Gulf of Trieste. The blue dot in the Gulf of Trieste inset indicates the location of Buoy Vida. Other toponym abbreviations are as follows: TS – Trieste (Italy), KP – Koper (Slovenia), PI – Piran (Slovenia), PO – Portorož Airport (Slovenia).

The Gulf of Trieste (GoT; Figure 1) is an open bay located at the northernmost limit of both the Adriatic and the Mediterranean Sea. Owing to its shallow depth (average depth of approximately 20 m), geographical position, and surrounding orogra-



phy, the GoT exhibits strong seasonal variability in both circulation and temperature (Malačić et al., 2006; Querin et al., 2021) and represents a classic region of freshwater influence (ROFI).

The mean circulation in the GoT follows the larger-scale Adriatic pattern and is predominantly cyclonic, with waters entering along the Istrian coast and exiting along the northern shoreline (Poulain and Cushman-Roisin, 2001). This circulation is strongly modulated by freshwater input from the Isonzo/Soča River, the main river discharging into the Gulf, with average discharges of around  $100 \text{ m}^3 \text{ s}^{-1}$ . The river maintains a persistent freshwater belt along the northern coast of the GoT and generates a pronounced north–south salinity gradient. During periods of high runoff, particularly in spring due to snowmelt within the river catchment, the Isonzo/Soča River can dominate over wind-driven dynamics, leading to river-induced circulation patterns (Cosoli et al., 2013; Lombardo et al., 2025). This enhanced discharge results in a basin-wide decrease in surface salinity, from typical winter values of 37.0–38.0 to summer values of 34.0–36.0 (Malačić et al., 2006; Russo et al., 2012).

Atmospheric forcing plays a key role in shaping the GoT dynamics. Strong northeasterly Bora/Burja winds represent the dominant wind regime, characterized by intense gustiness caused by hydraulic wave breaking (Grisogono and Belušić, 2009) over the Karst Plateau. The Bora/Burja, together with river discharge, constitutes the primary forcing of extreme circulation and mixing events in the Gulf (Lombardo et al., 2025). The second major wind regime is the Sirocco, a generally warm and moist southeasterly wind blowing over the Adriatic Sea, which is less gusty and often associated with precipitation events (Poulain and Raicich, 2001).

The seasonal interplay between freshwater input and atmospheric forcing governs the vertical structure of the water column in the GoT. During summer, calm conditions and enhanced river discharge promote strong stratification, with sea surface temperatures reaching values close to  $30 \text{ }^\circ\text{C}$ , while bottom temperatures typically remain around  $20 \text{ }^\circ\text{C}$ . The resulting pycnocline effectively insulates bottom waters from direct atmospheric heating. In contrast, during winter, frequent cold air outbreaks combined with strong Bora/Burja winds lead to intense surface cooling, enhanced evaporation, and increased water density. As a result, the water column becomes well mixed and temperatures commonly drop below  $10 \text{ }^\circ\text{C}$ . During extreme events, such as the cold spell of 2012, temperatures as low as  $4.2 \text{ }^\circ\text{C}$  were observed (Mihanović et al., 2013; Ličer et al., 2016; Carniel et al., 2016). These winter conditions allow for the formation of the coldest and densest waters of the Mediterranean Sea, which subsequently propagate southward into the deep Adriatic and further into the Ionian Sea, contributing to the ventilation of the Mediterranean basin (Gačić et al., 2001; Querin et al., 2013, 2016; Mihanović et al., 2019; Vodopivec et al., 2022; Martellucci et al., 2025).

At the ecosystem level, the large seasonal temperature range, and particularly the historically cold winter conditions, have shaped a unique marine biota adapted to this environment. However, rising winter temperatures in recent decades have facilitated the northward expansion of warm-water species, some of which threaten the balance of the local ecosystem (Mavrič et al., 2025b; Dulčić and Lipej, 2015; Lipej and Moskon, 2011). Therefore, in addition to increased thermal stress during summer, the native biota is increasingly challenged by invasive species that compete for resources and habitat (e.g., *Callinectes sapidus* - blue crab, *Mnemiopsis leidyi* - sea walnut). (Mavrič et al., 2025a; Rečnik et al., 2024; Fadeev et al., 2024; Lipej and Rogelja, 2021; Malej et al., 2017).



## 120 2.2 In situ measurements

The in situ surface salinity, surface temperature, bottom temperature and wind speed used in this study were obtained by the oceanographic buoy Vida (Malačič, 2019) and its predecessor COSP (Malačič et al., 2003). These data contain measurements from 2002 onward (Vodopivec et al., 2026). Vida is located in the Gulf of Trieste, 2 km offshore north-west from the cape Madona and the town of Piran (45°32.925' N, 13°33.042' E). The wind is measured using a 3D sonic anemometer WindMaster Pro from Gill Instruments, which is mounted on the buoy 5 m above sea level. A SeaBird SBE 16plus SEACAT CTD is mounted at 2.5 m depth and a Nortec AWAC AST 600 kHz acoustic Doppler current profiler (ADCP) with a temperature sensor is located at the bottom (21 m depth) in close vicinity. The ADCP is mounted to a tripod 0.5 m above the bottom (Cosoli et al., 2013). All the instruments are regularly cleaned and the CTD is calibrated every 6 months. Therefore, these instruments provide a reliable and almost uninterrupted data stream since autumn 2002.

125 Additional in situ data was provided by vertical CTD profiles which are obtained once to twice per month using a Sea&Sun free-falling microstructure CTD probe (MSS 90). The probe provides (among other parameters) high-frequency temperature and salinity measurements and a real-time water density value. The latter was used in the Brunt-Vaisala frequency calculation. The measurements were interpolated to regular 10 cm depth intervals and these values were used for the analysis. The CTD casts are performed since November 2007 and 692 profiles were used in the analysis. We used the profiles obtained at monitoring stations 000F (45.5381°N, 13.5454°E) and 00BF (45.4753°N, 13.6160°E), since both are in close vicinity to Vida buoy.

Precipitation and air temperature data were obtained from Portorož Airport automatic meteorological station. The station is located near the Sečovlje salt flats (45.4753°N, 13.6160°E, 2m above sealevel), about 2 km away from the sea and 10 km away from the Vida buoy. Daily values were downloaded from the Slovenian Environment Agency (ARSO) online archive (ARSO, 2025b). Air temperature for the 1994-2023 period was used to match the WMO guidelines (WMO, 2017) for at least 30-year time series requirement for climatological analysis.

Po daily runoff at Ponetalgoscuero station was obtained using the Arpae Dext3r data retrieval system (ARPAE, 2025). The data for for the 2003-2023 period was used in the analysis, matching the period of temperature and salinity data.

## 2.3 In situ data analysis

145 Salinity and surface and bottom temperature at Vida buoy are measured in 30 min intervals. We used these values to calculate daily averages which were then used in the further analysis. The multi-year averages and 90th percentile values were calculated using a 30-day moving window (Hobday et al., 2016) on the whole Vida dataset (2003-2023).

Detrending of the timeseries was not performed during climatological baseline calculation. The 2002-2023 dataset is shorter than the recommended 30-year period and there is less need for trend removal. Also removing the trend of the temperature timeseries makes sense if, for example, one wants to detect shifts in the frequency of MHW occurrences with respect to a moving baseline. This study on the other hand aims to analyze a given MHW event in the context of actual in situ thermal



stress on marine organisms. We therefore chose not to detrend as this removes the very real and persistent trend of ocean warming and its mounting pressure on those ecosystem communities which cannot adapt on the timescales of ocean warming.

Daily values were obtained for river Po runoff and Portorož Airport air temperature and a 30-day moving window was used on these datasets as well to calculate multi-year averages and the 10th and 90th percentile values.

The Brunt-Väisälä frequency was calculated using the density measured by the MSS90 probe. We used the values at 0.5m ( $h_1$ ) and 20 m ( $h_2$ ) depth in the calculation:

$$N^2 = \frac{g}{\rho_0} \frac{\rho(h_2) - \rho(h_1)}{h_2 - h_1} \quad (1)$$

Where  $g$  is the gravitational acceleration ( $g = 9.8 \text{ m/s}^2$ ) and  $\rho_0$  is the reference density ( $\rho_0 = 1025 \text{ kg/m}^3$ ). Therefore our stratification estimate is based on the assumption that the density change is linear, which is of course a very rough approximation, but still a good indicator of the stability of the water column. Monthly averages and 90th and 10th percentile values were calculated using (mostly) bi-monthly data.

## 2.4 Mixed layer depth estimation

A back-of-the-envelope calculation of the mixed layer depth (MLD, denoted as  $h$ ) at the location of the Vida buoy was performed using the wind stress - derived from measured wind speed, ERA5 air-sea heat fluxes and precipitation and measured river runoff. Deepening of MLD due to wind stress is derived following Cushman-Roisin and Beckers (2011), using the change in potential energy when mixing a stratified water column of mixed layer depth  $h$ :

$$E_P = \frac{1}{12} \rho_0 N^2 h^3 \quad (2)$$

which is caused by the work performed by the wind stress  $\tau = \rho_a C_D u_w^2 = \rho_0 u_*^2$ :

$$\frac{dE_P}{dt} = m \rho_0 u_*^3 \quad (3)$$

The change in MLD related to the wind stress can therefore be written as:

$$dh = \frac{4m}{N^2 h^2} \left( \frac{\tau}{\rho_0} \right)^{3/2} dt \quad (4)$$

In the above equations,  $u_w$  is the wind speed,  $u_*$  is the turbulent friction velocity,  $\rho_0$  is the reference water density ( $\rho_0 = 1028 \text{ kg/m}^3$ ),  $\rho_a$  is the air density ( $\rho_a = 1.293 \text{ kg/m}^3$ ),  $C_D$  is the wind drag coefficient ( $C_D = 1.1 \cdot 10^{-3}$ ) and  $m$  is the coefficient of proportionality that accounts for the rate of work performed by the wind stress minus the portion diverted to kinetic energy production ( $m = 1.25$ ). Note that this approach to mixed layer entrainment calculation is somewhat questionable as it is based on energy transfer instead of mean momentum constraint (Umlauf and Burchard, 2005; Large et al., 1994; Price, 1979). However, we are looking just for a rough estimate and, as we'll show in the next section, it managed to produce solid results.



180 On the other hand, the buoyancy flux ( $B$ ) can destabilize or stabilize the water column. Following Marshall and Schott (1999) the change in MLD is given by:

$$dh = \frac{-B}{N^2 h} dt \quad (5)$$

The buoyancy flux consists of the heat flux and freshwater terms (Gill, 1982):

$$B = \frac{g\alpha Q_{\text{net}}}{\rho_0 C_w} - g\beta S(E - P - R) \quad (6)$$

185 Where  $\alpha$  is the thermal expansion coefficient ( $\alpha = 2 \cdot 10^{-4} \text{ K}^{-1}$ ),  $C_p$  is the specific heat capacity ( $C_w = 3990 \text{ J/kgK}$ ) and  $Q_{\text{net}}$  is the net surface heat flux.  $\beta$  is the haline contraction coefficient ( $\beta = 7.6 \cdot 10^{-4}$ ),  $S$  is salinity,  $E$  is the evaporation rate,  $P$  is precipitation rate and  $R$  is river runoff divided by the surface area of the Gulf of Trieste ( $550 \text{ km}^2$ ). Note that that in our case the second term is negative (contrary to Gill (1982)) since evaporation reduces buoyancy and heat flux is positive downwards and therefore increases buoyancy.

190 In our estimates we used the net heat flux, evaporation and precipitation from the ERA5 atmospheric reanalysis (Hersbach et al., 2020). Values from grid cells that are marked as at least 60% water in the ERA5 land-sea mask were used and averaged over the Gulf of Trieste area. Isonzo/Soča and Rižana monthly discharge was obtained from Slovenian Environment Agency (ARSO, 2025a) measured at Solkan and Dekani stations respectively.

The most poorly known parameter in our MLD calculations is the Brunt-Väisälä frequency ( $N$ ). Since there are no contin-  
195 uous salinity measurements at the bottom,  $N$  was based on vertical CTD profiles, which are quite sparse. This means that a bottom density value - and consequently the Brunt-Väisälä frequency - was measured only on 16 different days in 2023.

Summing the deepening and shoaling of the mixed layer, the MLD equation in its final discrete form is:

$$h_n = h_{n-1} + \frac{4m}{N^2 h_{n-1}^2} \left( \frac{\rho_a C_D u_w^2}{\rho_0} \right)^{3/2} \Delta t - \frac{g\alpha Q_{\text{net}}}{\rho_0 C_p N^2 h_{n-1}} \Delta t + \frac{g\beta S(E - P - R)}{N^2 h_{n-1}} \Delta t \quad (7)$$

200 We used the hourly measurements of wind speed and hourly reanalysis of heat flux, evaporation and precipitation in our calculations and therefore the time step used was  $\Delta t = 1$  hour. The MLD value ( $h$ ) was limited between 3 m and 22 m (bottom depth).

## 2.5 Modelling component

In order to integrate the observations and obtain a basin-wide picture of the event, we developed a series of high-fidelity simulations of the Gulf of Trieste. For this purpose, the MITgcm finite volume numerical model (Marshall et al., 1997) was  
205 implemented twice. The first simulation covered the northern Adriatic Sea, defined as the portion approximately north of the Ancona-Zadar line (see Figure 1 for NAd model domain), spanning the entire year 2023, with an integration time step of 100 s and hourly average output. The domain was discretized into rectangular cells on an Arakawa C grid, with a horizontal spacing of  $1/128^\circ$  (about 750 m), while the vertical levels were characterised by uniform height (1 m) in the topmost 20- m layer, and then progressively thicker (up to 11 m) with depth. The atmospheric forcing was derived from a sequence of 3-day



210 forecasts provided by the COSMO-2I weather model (<https://www.arpae.it/temi-ambientali/meteo/>), while initial and open  
boundary conditions (on the southern side of the domain) were obtained from the Mediterranean Physics Analysis and Forecast  
products (Escudier et al., 2024) distributed by the Copernicus Marine Service (CMS). We considered 19 rivers whose flow was  
calculated with a seasonally modulated climatology, except for the Po, Isonzo/Soča and Timavo rivers, for which hourly data  
were available, collected at the Pieris hydrometric station, made available by the Regional Agency for Environmental Protection  
215 (ARPA FVG). The riverbeds near the estuaries were simulated as straight channels of uniform depth, from which velocities  
were imposed as boundary conditions to the model (Querin et al., 2021). A second simulation encompassing the Gulf of Trieste  
was nested ( one-way ) into the former one: the boundary conditions were interpolated from the NAd parent run on the higher  
resolution grid, with a six times higher horizontal spacing of  $1/768^\circ$  (about 125 m) and vertical thickness of 0.5 m for the  
topmost 6 layers, then of 1 m in the interior and of 2 m to the deepest ( $\geq 32$  m) layers. The integration time step was set to  
220 10 s, to ensure numerical stability even during very high riverine flow rate events. The outputs (averages) were saved at hourly  
intervals. The high vertical resolution of both parent and nested simulations allows for a more accurate description of the  
stratification or mixing, the latter being parameterized by the turbulent kinetic energy (TKE) based scheme of (Gaspar et al.,  
1990), to better capture the possible causes of the heat wave we investigated. In addition, a longer run (5 years, from 2017 to  
2021) was available for the northern Adriatic Sea, set up with the same configuration as the parent 2023 simulation (Giordano  
225 and Querin, 2025). This was used as a “climatological” reference to determine whether the patterns observed in the 2023 runs  
were anomalous compared to previous years. Hereinafter we will refer to the 2023 northern Adriatic parent run as “NAd”, to  
the nested Gulf of Trieste one as “GoT” and to the reference one as “5yrs”.



### 3 Results

#### 3.1 In situ data

230 At the start of the year 2023 the bottom temperature was above the 90th percentile and would therefore already classify as a heatwave (Hobday et al., 2016). However, it fell below the threshold value before the end of January and stayed slightly (0.5°C to 1°C) above multi-year average through the whole spring and first part of the summer period. On the 5th of August the measured daily value crossed the 90th percentile threshold again and stayed above that until the 21st of November (Figure 2). During this period, the daily bottom temperature dropped below the 90th percentile threshold only twice, namely on the 9th of August and on the 9th of November, therefore qualifying as a three and a half months long bottom heatwave (BMHW) (Hobday et al., 2016; Amaya et al., 2023a). The observed bottom heatwave was of unprecedented intensity with daily temperatures up to 4.3°C above the long time average. The maximum daily bottom temperature in 2023 was 24.7°C, which is 1.2°C above the highest daily bottom temperature ever recorded at the Vida buoy and a full 4.1°C above the highest climatological value (average daily bottom temperature).

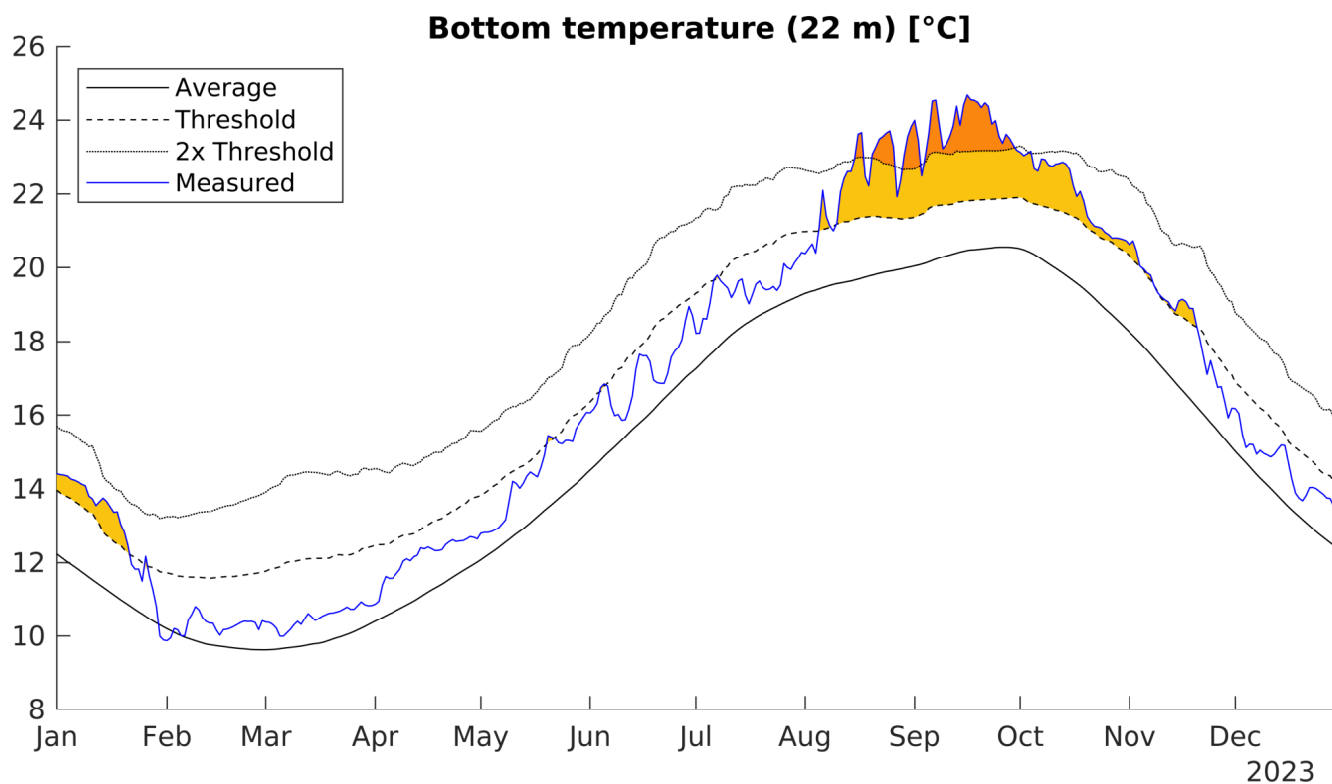


**Figure 2.** Measured bottom temperature (blue line) at the location of Vida buoy. Solid black line represents a long time average, the dashed black line represents the 90th percentile, and dotted black line represents twice the difference between the average and 90th percentile. The former two represent category I and category II heatwaves following (Hobday et al., 2018).



240 Meanwhile, the measured sea surface temperature at the same location was above average as well throughout the period, but exceeded the 90th percentile only in the periods from the 15th of July to 25th of July and in the period from the 21st of August until the 29th of August (Figure 3). Another surface heatwave started on the 11th of September and lasted until the end of the year. However, the significant overheating of the surface layer started only after the bottom heatwave was already in progress. In fact, in the beginning of August when the BMHW started, there was a significant drop in surface temperature which came close to the multi-year average. Fascinatingly, when the long SMHW started in September, the surface temperature was quickly 245 matched by the bottom temperature.

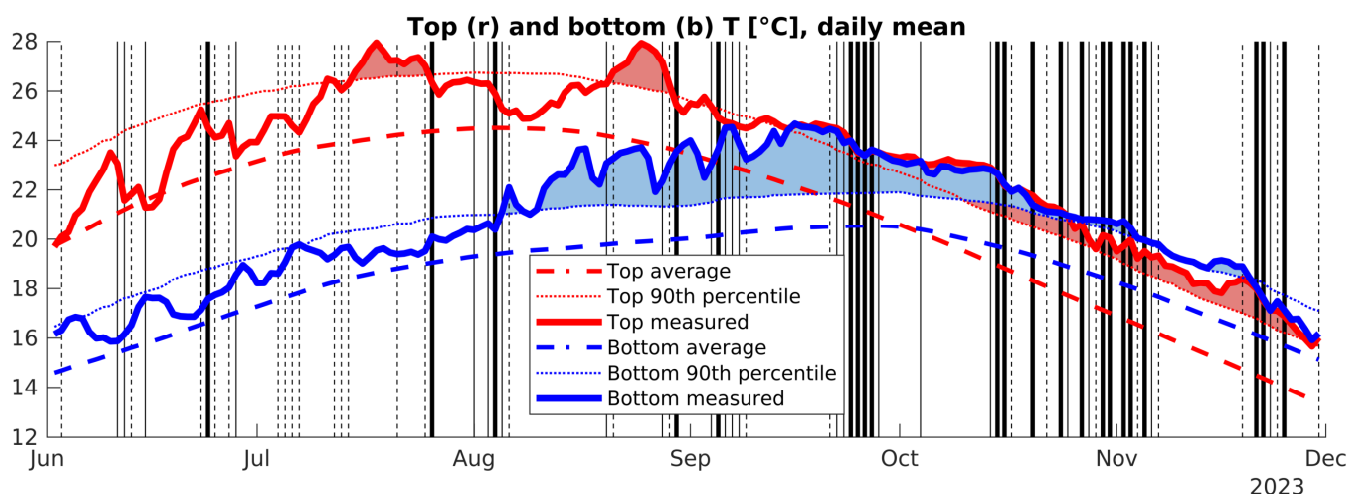


**Figure 3.** Measured surface (red) and bottom (blue) temperature at Vida buoy for the period from July 2023 to November 2023. Black vertical lines mark days with average wind speed above 4 m/s (thin dashed), above 5 m/s (thin) and above 7 m/s (thick).

Looking at the salinity plots (Figure 4) we observe that the year 2023 started with unusually high surface salinity which stayed above or around 90th percentile value most of the time until mid September. There are several short-lived drops in salinity which often correlate with precipitation events. These are marked with vertical blue lines in Figure 4: thin dashed lines 250 marking events with more than 1 mm daily precipitation, thin solid lines marking days with more than 5 mm and thick solid lines marking days with more than 10 mm precipitation. The extremely high salinity was a consequence of a long drought period which is reflected in the Po runoff (Figure 5). The latter was below the 10th percentile value most of the time in 2022 and in the beginning of 2023. There is a short sharp peak in runoff at the end of May 2023, but that drops again quickly below the average value. It stays below average throughout the summer followed by several peaks in the autumn.

255 The exceptionally high surface salinity should result in a reduced stratification of the water column. This is indeed clearly shown in Figure 6 through very low values of Brunt-Väisälä frequency ( $N^2$ ) during all the CTD casts in 2023 (shaded), as compared to the values of  $N^2$  during other years in the period 2019 - 2024.

The red dots in the bottom panel in Figure 4 show the Brunt-Väisälä frequency obtained from CTD casts during 2023. Unfortunately the CTD probe was undergoing maintenance through June and July and we are missing the  $N^2$  values in that

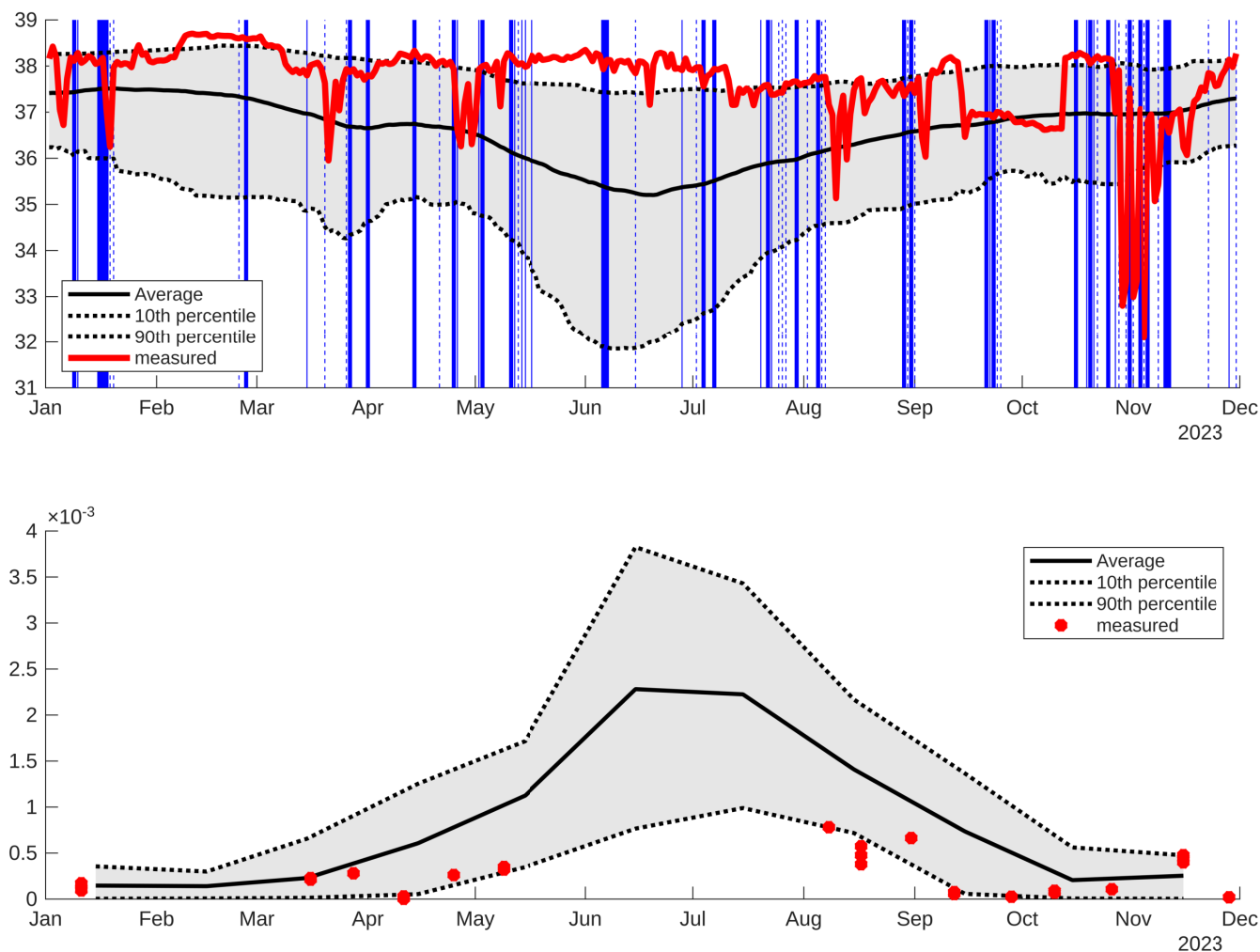


**Figure 4.** Top: Measured surface salinity. Blue w lines mark days with precipitation over 1 mm (thin dashed), over 5 mm (thin) and over 10 mm (thick). Bottom: Brunt-Väisälä ( $N^2$  in  $s^2$ ) frequency from CTD casts.

260 period. However, we can see that the values from April to November are mostly around the 10th percentile value, so the frequency and therefore stratification were extremely low in that period. That would lead us to the speculation that the wind in summer 2023 was able to mix the water column much deeper than usually in this period of the year. The black vertical lines in Figure 3 indicate high wind events. The days with average wind speed above 4 m/s are marked with thin dashed lines, those with average wind speed above 5 m/s are marked with thin solid lines and those above 7 m/s are marked with thick solid lines.

265 In the top panel we can see that high wind events are often followed by a jump in bottom temperature, indicating that the mixed layer deepened enough to affect the bottom waters (e.g. 4th to 6th of August, 28th to 31st of August, 3rd to 7th of September, etc.).

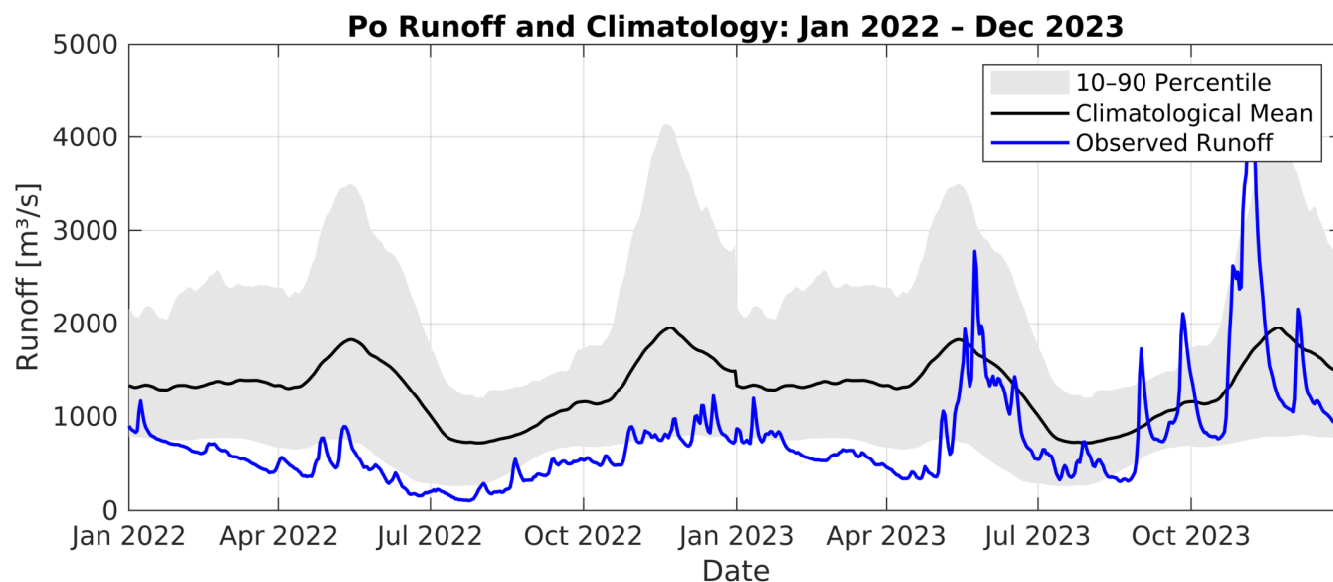


**Figure 5.** Po runoff for 2022 and 2023. The climatology was calculated on a 2003-2023 period using 30-day running average.

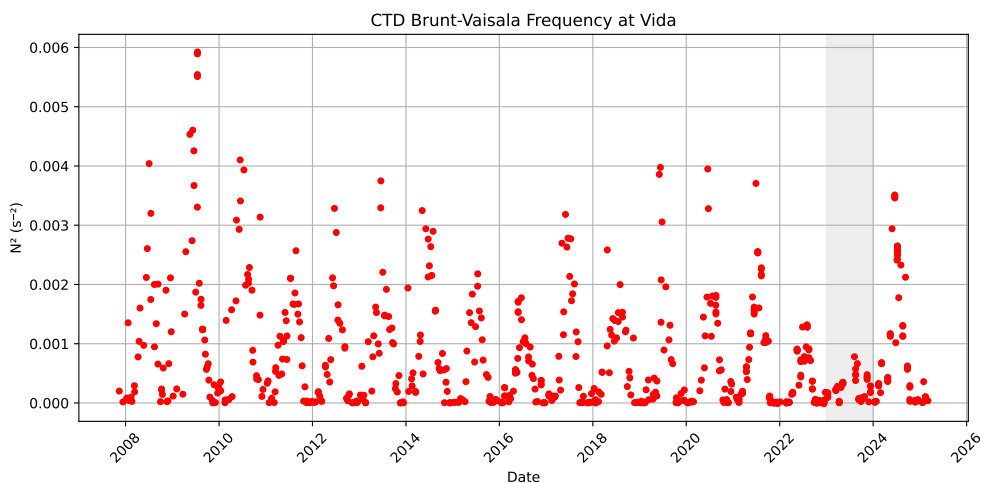


**Figure 6.** Brunt-Väisälä frequency ( $N^2$  in  $s^{-2}$ ) computed from CTD casts at the location of Vida buoy in the period 2008-2024. The gray area marks the year 2023.

We estimate the mixed layer depth (MLD) using the equation (7). Since we don't have enough CTD casts, we assume that  $N^2$  was at the 10th percentile value all of the time. This is a very rough assumption based on the results shown in Figure 4. However, the whole MLD calculation is very approximate and should serve only to help us estimate whether the conditions allowed for wind mixing of the whole water column. The results shown in the top plot in Figure 7 are encouraging. The blue

270



dots are MLD values visually derived from the observed CTD profiles (Supplementary material) and the calculated MLD (thick red curve) matches the observed MLD depth quite well. This gives us the confidence that the back-of-the-envelope calculation (section 2.1) was justified. The thin red line marks the MLD calculated with average  $N^2$  (instead of the 10th percentile value).  
275 This is an estimate of MLD as it would have been if the stratification were 'normal', i.e. there was no drought preconditioning causing the high salinity.

The ellipses mark three important MLD events. The first one in May (marked with no. 1) shows deepening down to the bottom, and this is also reflected in the temperature plot (Figure 7 bottom), where bottom temperature matches the surface temperature which indicates a fully mixed column. The event no. 2 happens in the first days of August, when the BMHW  
280 started. The MLD reaches 15 m depth and the deep mixing is reflected in the rise of bottom temperature from 20.4°C to 22.1°C. This deepening started the extreme overheating. On the other hand, the thin red line deepens to only 8 m confirming that the BMHW would not have happened if the stratification was higher. The third ellipse (no. 3) marks two consecutive deepenings of the MLD which are both reflected in the rise of the bottom temperature. The first deepening doesn't quite reach the bottom (MLD reaches 18 m depth), however, the bottom temperature rises from 21.9°C to 24°C. The second deepening  
285 reaches the bottom and again this is reflected in a match between the surface and bottom temperature. The latter rises from 22.5°C to an unprecedented 24.5°C.

There are oscillations in bottom temperature between the events marked as no.2 and no.3 in Figure 7. We can observe sharp drops and then sudden rises which can't be explained with changes in MLD, however the model results provide a better insight and a reasonable explanation (see section 3.2).

290 At the end of October the bottom temperature surpasses the surface temperature and stays higher for about a month (Figure 3). A look at surface salinity measurements (Figure 4) shows that the event coincides with a sudden drop in salinity, which reaches even below the 10th percentile value. After a prolonged drought period, the end of October brought high precipitation - also visible in the Po discharge (Figure 5) - and the large amounts of freshwater re-stratified the column. This prevented the cooler surface layers to mix down to the bottom and effectively trapped the heat in the bottom layers, prolonging the BMHW  
295 for another month.

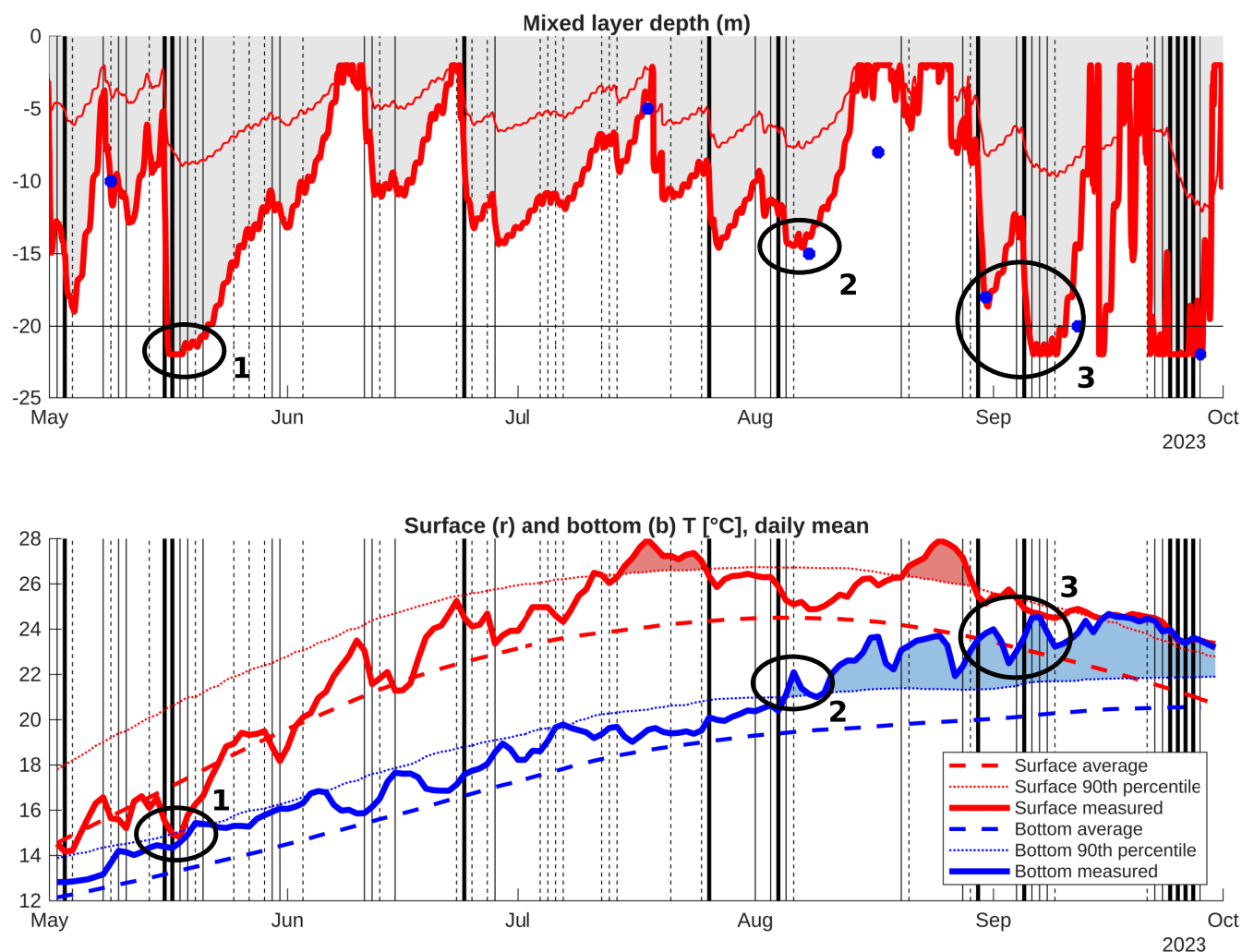


**Figure 7.** Top: Estimated mixed layer depth at the Vida buoy (gray area and thick red line). The blue dots represent the mixed layer depth observed in CTD profiles at the location of the Vida buoy. Black vertical lines mark days with average wind speed above 4 m/s (thin dashed), above 5 m/s (thin) and above 7 m/s (thick). The thin red line represents the MLD calculation using an average  $N^2$  value - the MLD if stratification was 'normal', without drought. Bottom: Surface (red) and bottom (blue) temperature measured at Vida buoy (same as Figure 3). Vertical lines represent windy days (same as MLD plot). Ellipses mark important MLD deepening events described in the text.



### 3.2 Model results

From the simulated field of temperature from the nested “GoT” we extracted the time evolution of the vertical profile corresponding to the grid cell nearest to the Vida buoy coordinates (45.54875 °N, 13.55070 °E), shown in Figure 8. Comparing the “GoT” simulated sea surface temperature with the Vida buoy data shows good agreement throughout the year, except for the period between May and June, where the model presents a colder bias, reaching up to 5 °C at some points. After that however the GoT temperature picks up and matches again with the observations, starting from July and for the remainder of the year. Vida data aligns quite well also with L3 SST from satellite (Pisano et al., 2024) as well as from the Copernicus Marine Service Mediterranean Physics Analysis and Forecast (MFS). Since the latter assimilates satellite observations the closer agreement with surface data is to be expected, when compared to the free MITgcm run.

In the bottom layer instead, the MFS and MITgcm runs both show large discrepancies with respect to the Vida data. The former presents a steady increase in temperature, almost linear at a rate of more than 3°C/month, overestimating the peak temperature at almost 27°C and with bias reaching up to almost 5°C. The latter instead shows a similar trend as we highlighted at the surface: a colder bias during spring and the beginning of summer, with a sudden increase which almost matches the observed temperature. In this case we observe a delay in this rising: at the surface it occurred at the beginning of to mid July, while at the bottom is localised at the beginning of August. The MITgcm run also shows a much larger variability, much closer to the one in the observational data.

We extracted the closest grid cell to the Vida location also for the parent simulation “NAd”, and the corresponding “5yrs” run spanning from 2017 to 2021, as described in section 2.5. In Figure 9 we report these outputs.

Comparing the nesting child and parent simulations, we observe little differences in the temperature time series, with the larger discrepancies in the deepest layers. We can therefore confidently compare the GoT run with the averaged reference one: the 2023 simulated summer surface temperature sits in the standard deviation band of the reference run, only overcoming it by the end of September. On the contrary, in the deeper layers the discrepancy is evident: looking at the 19.5 m time series, temperatures increase sharply by almost 5°C at the beginning of August. The simulation thus confirm the observed signal: 2023 was not an exceptional year with respect to the previous one in terms of surface temperature, but it was when looking at the bottom. The GoT Hovmöller diagram reveals how the strong and sudden heating well aligns with tongues of warm water descending from the surface at the beginning and end of August, hinting at an extreme penetration of heat from the topmost to the bottom layers.

We show analogous plots but for salinity in Figure 10. Again, parent and nested runs present small discrepancies, so we can compare them equally to the 5yrs simulation. Doing so we observe how 2023 was consistently saltier all along the water column, with only sporadic events of fresher water than the reference run, as values exceeded the previous years’ average by more than one standard deviation most of the time. The Hovmöller diagram further strengthens this, showing how from July almost till November the whole water column as a mostly uniform salinity, with fresh water confined to the upper 5 to 10 m in short events, while high values, up to 39, extend down to 15 m depth, persisting for some days.



The deep mixing is also noticeable in Figure 11: up until mid July the mixed layer depth, computed by the model based on  
330 a temperature threshold criterion (Kara et al., 2000), mostly stays around 5 m, occasionally reaching 10 m. At the end of July  
the model MLD starts to deepen and in the beginning of August it descends to more than 15 m - coinciding with the beginning  
of the BMHW and also with the event no.2 in the theoretical MLD calculation (Figure 7). The model MLD in this event is  
somewhat deeper than the theoretical estimate. The double deepening at the end of August and in the beginning of September  
(Figure 7 - event no.3) can be observed in the model results as well. This time the model MLD is slightly shallower than the  
335 theoretical estimate, however the similarity of the event is obvious and the deepening is reflected in the rise of measured bottom  
temperature.

Figure 12 shows the anomaly between the GoT and 5yrs runs of temperature at 20 m depth, with daily averages spanning  
from July to October. From these we observe how the Vida buoy observations reflect the conditions of the entire Gulf. In July  
temperatures are actually below the 2017-2021 average, as the warming appears from the end of the month outside the Gulf of  
340 Trieste, to then propagate inside during August, persisting in September and October. A slightly colder anomaly is sometimes  
found at the centre of the Gulf, related to the average cyclonic circulation of the basin.

From these time frames it is not clear whether the heat wave measured by the Vida buoy was the effect of warm waters  
coming from outside the domain, as the strong positive anomalies of August and September seem to suggest. Figure 13 shows  
the vertical profiles along the transect (yellow line in the first panel fo Figure 12) of daily average temperature. Along the ~  
345 15 km transect no clear advection of deep warm waters is visible; on the contrary, starting from the relatively cool condition at  
the beginning of July, the heating appears uniform, starting from the surface and penetrating to the deeper layers by the end of  
August.

The mesoscale variability of the cold eddy structure (see Figure 12) can also explain the bottom temperature oscillations  
visible in Figure 7 (bottom plot - blue solid line), between August and September. Figure 14 shows maps, at 20 m depth, of  
350 simulated temperature for different days. These are accompanied by the corresponding value extracted from the Vida buoy  
nearest grid cell along the model's timeseries from August 7<sup>th</sup> to September 14<sup>th</sup>. From these, the temperature oscillations  
appear to be correlated with the variability in position and intensity of the cyclonic eddy. When it moves closer to the Vida  
buoy (location marked with a green cross), the simulated temperature decreases (e.g. on August 15<sup>th</sup>); when the cold anomaly  
weakens warmer water intrudes, increasing temperatures to more than 24 °C (e.g. on September 5<sup>th</sup>); when the eddy regains  
355 intensity, again temperature drops, almost by 1 °C (on September 8<sup>th</sup>).

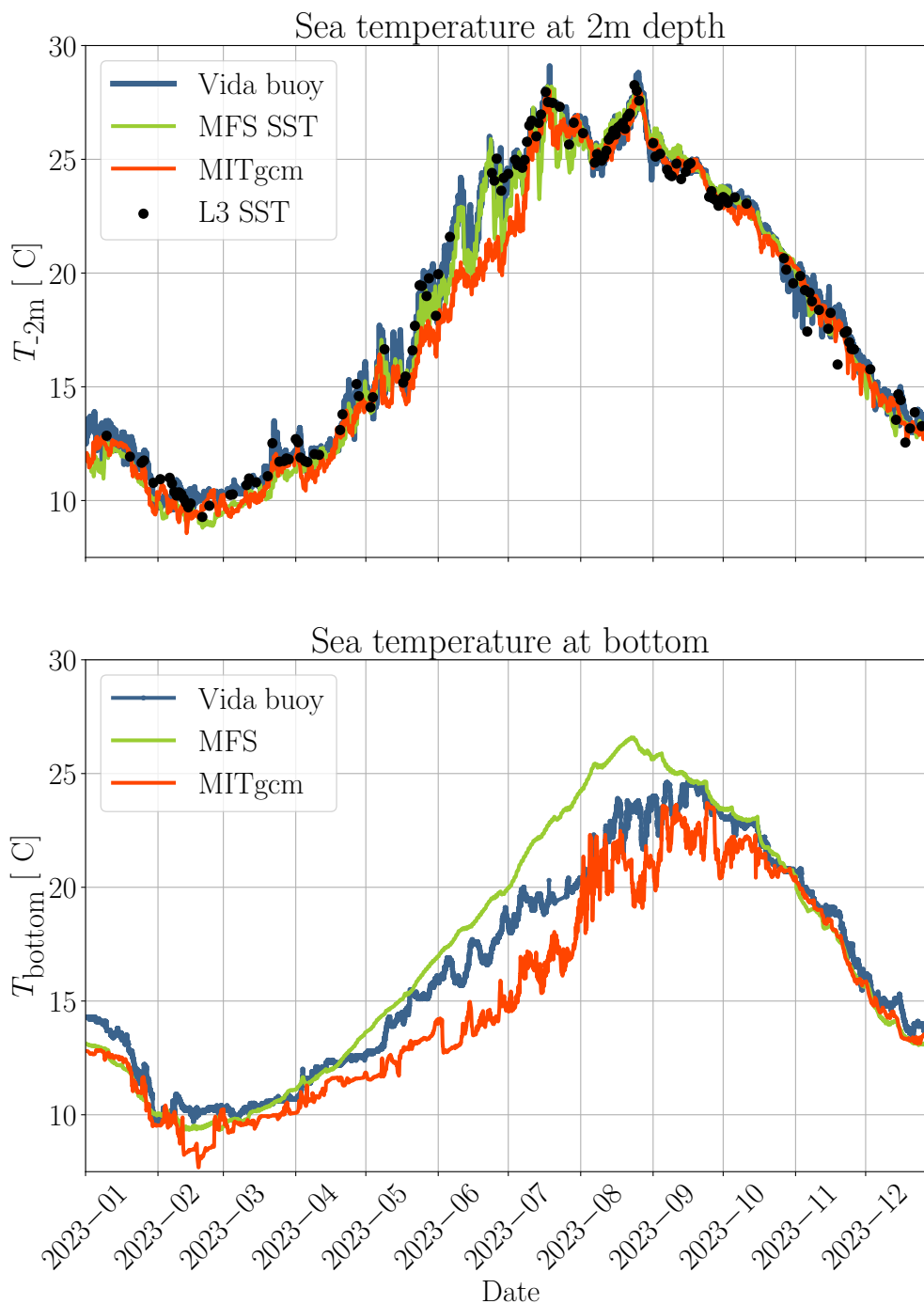


**Figure 8.** Upper panel: time series of sea surface temperature as measured by the Vida buoy compared with satellite L3 SST, Copernicus Marine Mediterranean Physics Analysis and Forecast (MFS) and the MITgcm run. Lower panel: same for the bottom temperature.

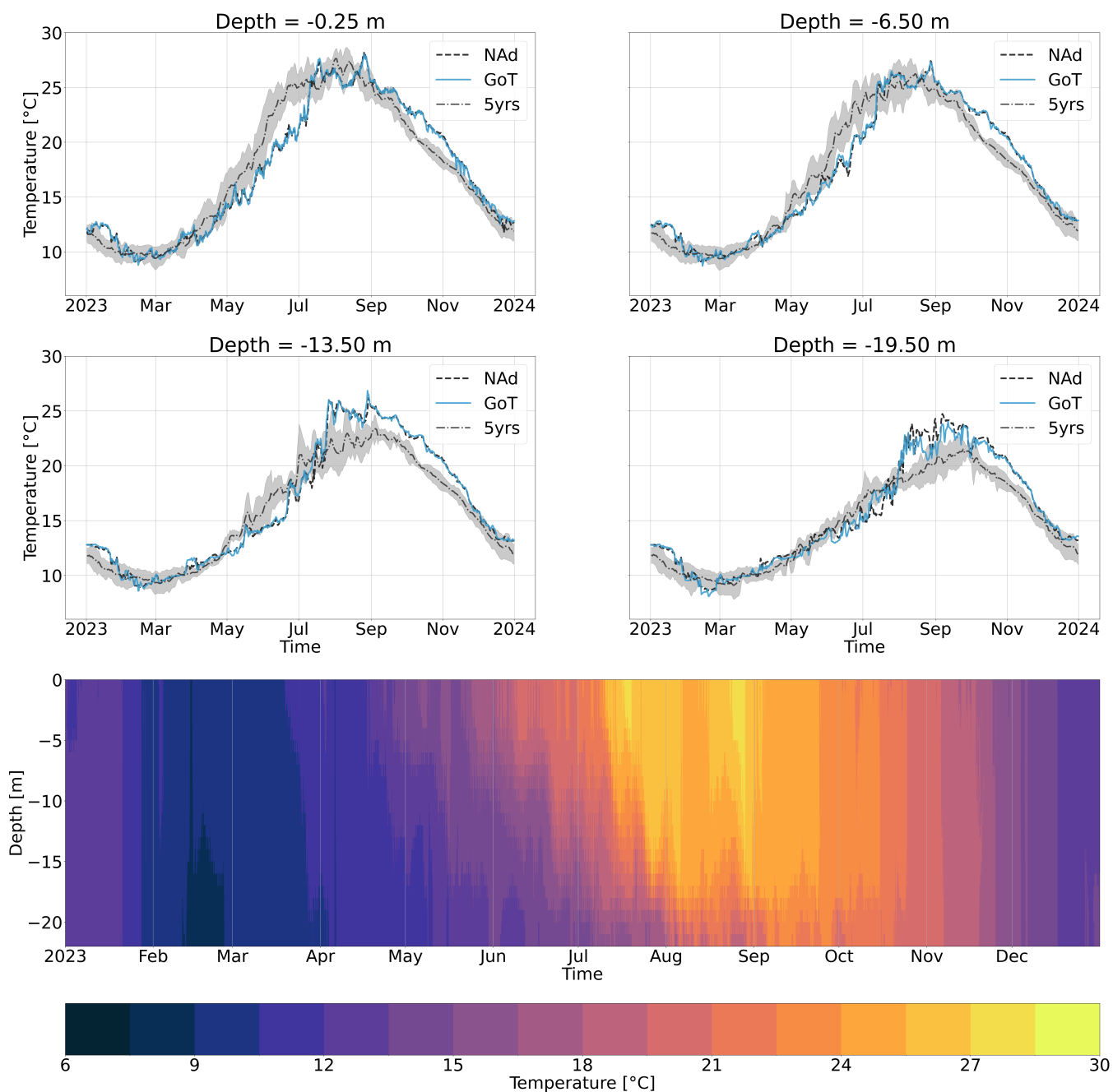


**Figure 9.** Upper panels: time series of temperature at different depths; for each panel the parent (“NAd”), nested (“GoT”) and reference run over the northern Adriatic (“5yrs”, also with standard deviation band) are shown. Lower panel: Hovmöller diagram of temperature.

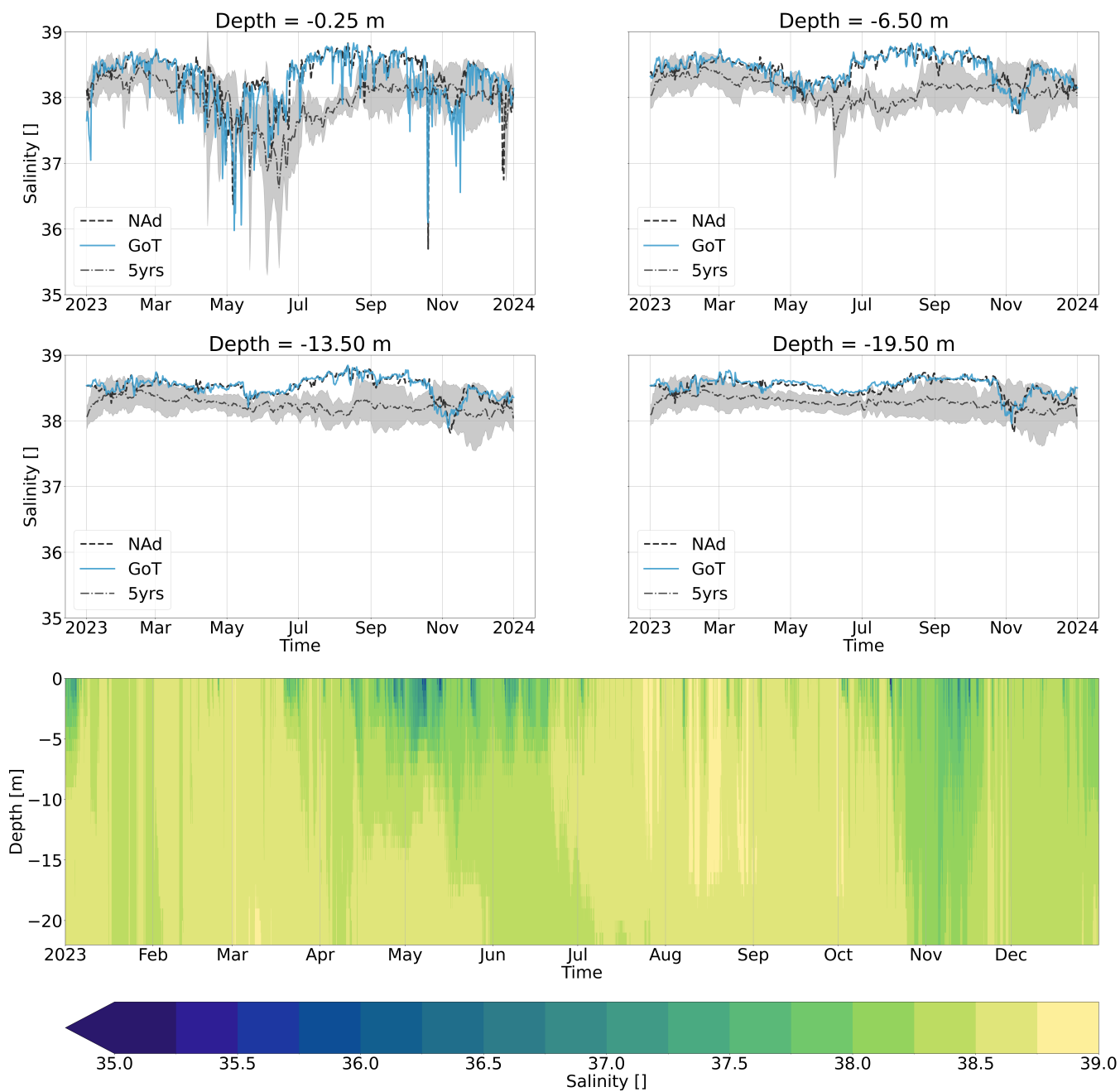


**Figure 10.** Upper panels: time series of salinity at different depths; for each panel the parent (“NAd”), nested (“GoT”) and reference run over the northern Adriatic (“5yrs”, also with standard deviation band) are shown. Lower panel: Hovmöller diagram of salinity.

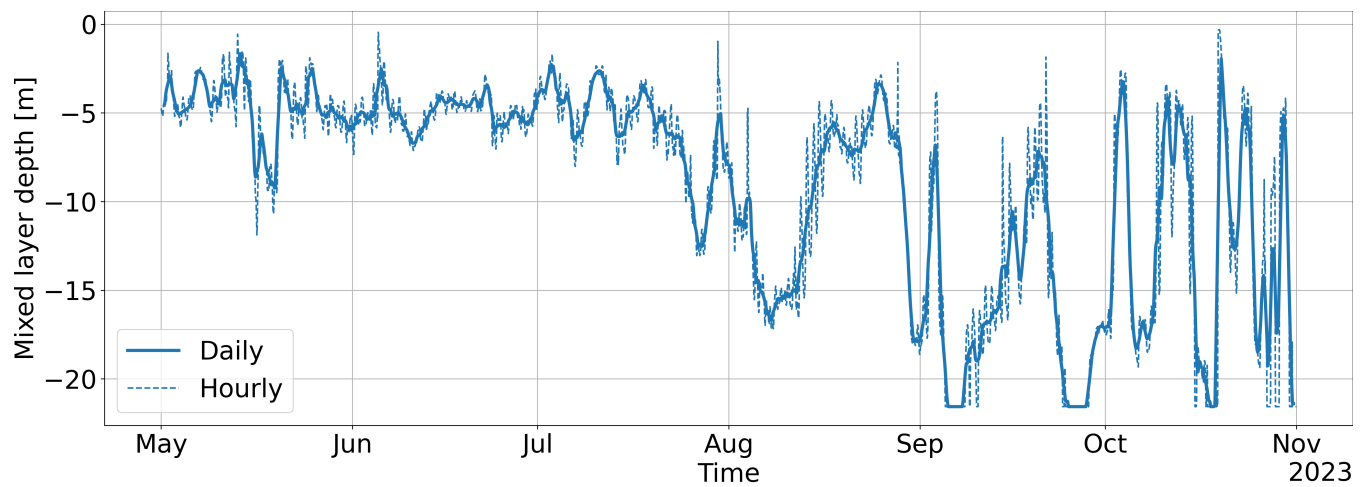


**Figure 11.** Mixed layer depth as simulated by the GoT run at the Vida buoy coordinates, from May to October; hourly (original MITgcm output) and daily (moving window) values.

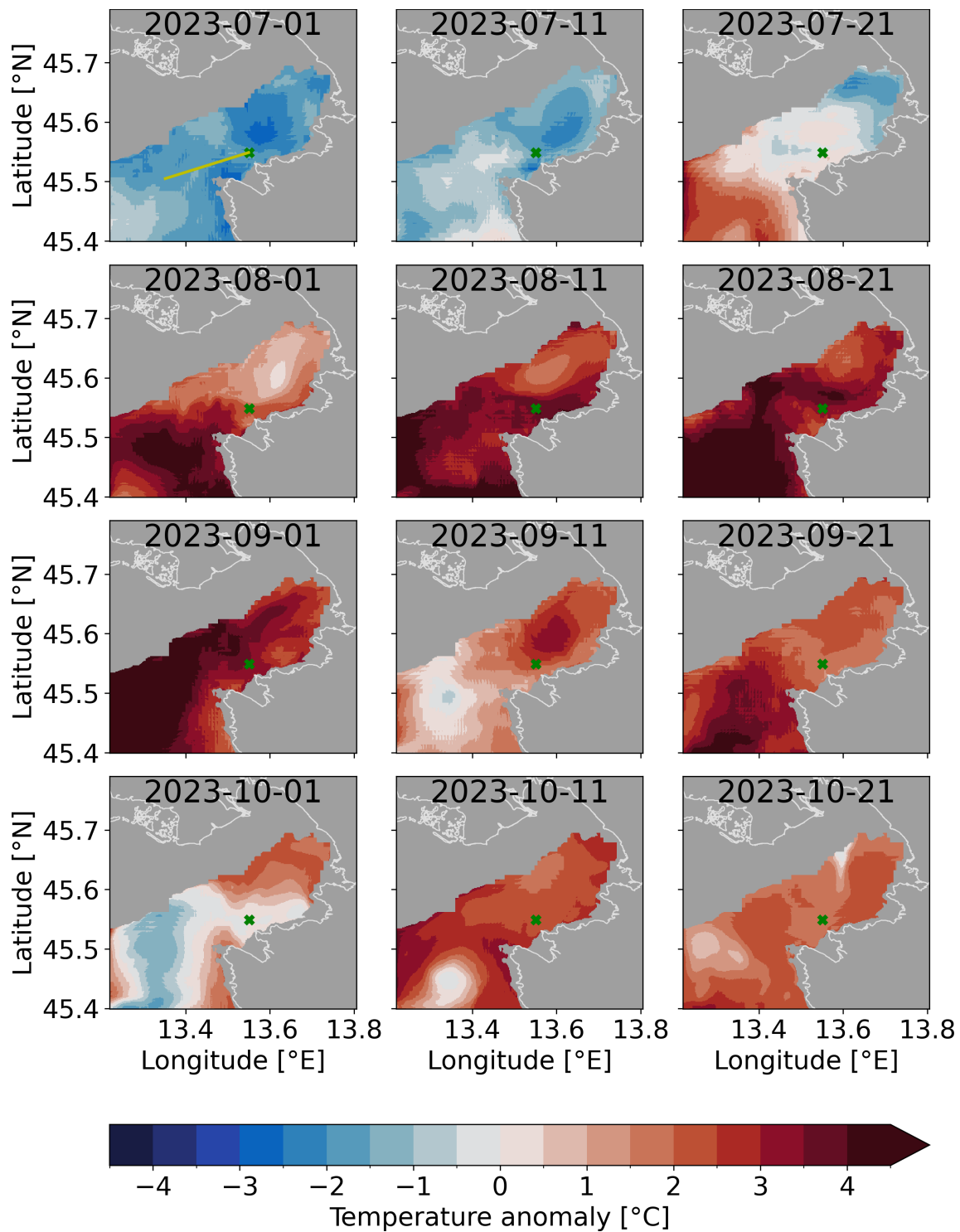


**Figure 12.** Average daily anomaly of 20 m temperature between the GoT and 5yrs runs; the cross indicates the Vida buoy position, the yellow line the transect of Figure 13.

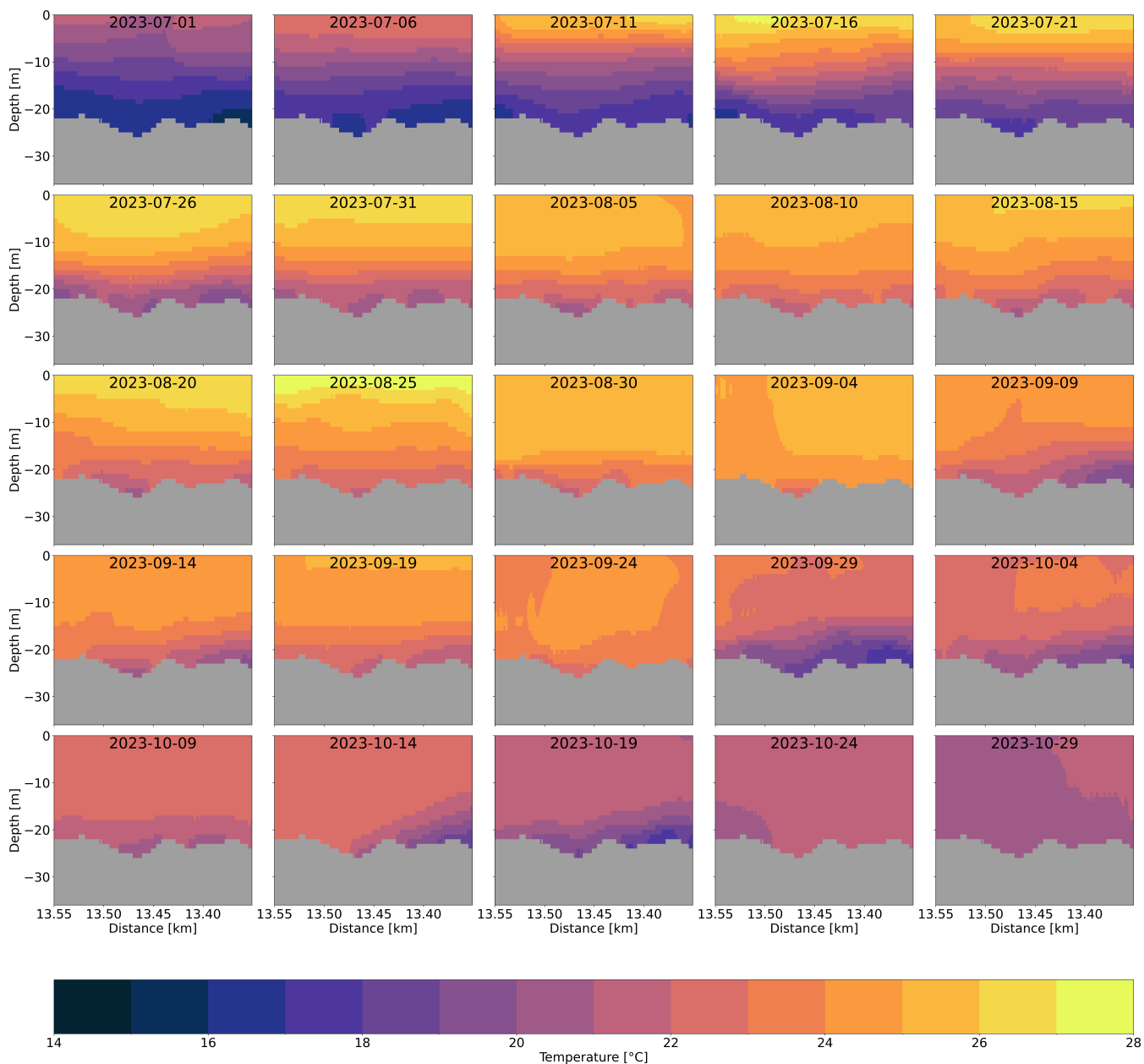


**Figure 13.** Vertical profiles of average daily temperature along the transect shown in Figure 12; distance from the Vida buoy on the abscissa, so that its position stands at the right of each plot.

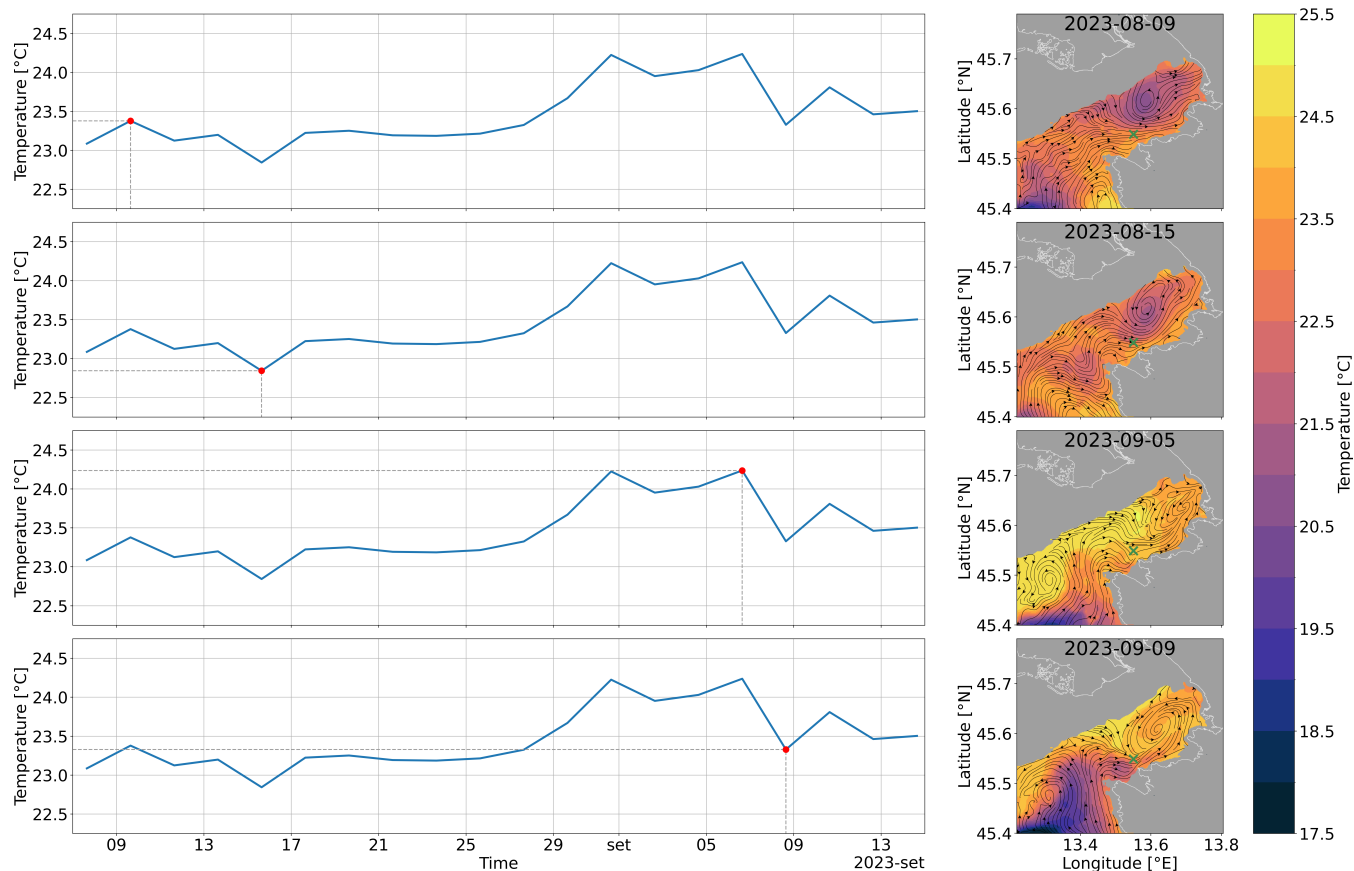


**Figure 14.** Right panels: 20 m depth daily average temperature maps during four selected days between August and September. Location of the Vida buoy is marked with a green cross. Left panels: simulated timeseries at the Vida buoy nearest grid cell, from August 7<sup>th</sup> to September 14<sup>th</sup>; days corresponding to the maps on the right are highlighted with a red dot.



#### 4 Discussion

The MHW guidelines (Hobday et al., 2016; Amaya et al., 2023a) recommend using a 30-year baseline as a reference. However, long term bottom temperature observations are extremely scarce and the 22-year-long dataset from buoy Vida provides a rare opportunity for one of the rare in situ observations of a BMHW.

360 The measurements showed that, while the surface temperatures were above average but aligned with recent trends, the bottom temperature exceeded by far any previous record, with peaks up to 24.7°C and overall a heat wave persisting for more than three months. Conductivity measurements also revealed a long track of exceptionally high salinity throughout the end of 2022 and all of 2023, correlated with a period of low discharge from the Po, the main river flowing into the Adriatic Sea. This suggests a preconditioning of the region, including the Gulf of Trieste, where high salinity caused a reduced stratification of  
365 the water column that made it more susceptible to propagate heat towards the deeper layers. This hypothesis is reinforced by the low Brunt-Väisälä frequency and the calculated deepening of the mixed layer (computed using the observational dataset and model simulations) reaching 20 m depth.

There is an ongoing discussion whether the baseline temperature and thresholds should be detrended when calculating MHW and BMHW statistics, especially in areas with strong warming trends (Capotondi et al., 2024; Amaya et al., 2023a, b). Due to  
370 a shortened baseline period (22 years instead of 30 years) there was less need for such an approach and the de-trending was not performed. The use of 10th percentile value of Brunt-Väisälä frequency in our MLD calculations is somewhat disputable due to lack of CTD casts in June and July. However, extremely high salinity measurements at the surface during this period, justify our choice.

A nested numerical simulation allowed us to fill the blanks where data are not available, giving us a full picture of the  
375 dynamics of the Gulf of Trieste in 2023. Albeit with some cold bias during spring, the model seems capable of reproducing the observed signal, in particular at the bottom where it outperforms the larger scales Copernicus Marine Forecast and Analysis. This gives us the confidence in using the simulation to study the heat wave. Looking at the 20 m depth temperature the observed signal reflects a wider condition, with deep waters suddenly heating, up to 4°C more than a reference run. This signal is present even outside the Gulf and seems to occur there slightly before the onset of the heat wave as recorded by the Vida buoy. A  
380 synthetic transect helped us to discern the origin of this event. It did not show evidence of the advection of deep warm water from outside the Gulf, instead it supports the preconditioning hypothesis: the heating happened uniformly along the transect, starting from the surface and warming the deeper layers. It is hinting thus at an atmospheric origin for the event, similar to surface heat waves, that instead, owing to the reduced stratification preconditioning, propagated vertically reaching the bottom of the Gulf.

385 The comparison between observations, Copernicus Mediterranean Forecast and Analysis and MITgcm run highlighted the improved performance of the latter in reproducing the bottom temperature evolution. Therefore, the very high model horizontal and vertical resolution proves crucial to study and monitor such extreme events. We also stress that the MITgcm runs were free hindcasts, with no data assimilation except for the indirectly included one at the open boundary of the NAd simulation and in



the initial conditions; a data assimilating, high resolution modelling framework would be even more skilled in reconstructing  
390 and possibly monitoring and predicting bottom marine heatwaves.

The results of this work are in line with modelling studies of MHWs and BMHWs in the Mediterranean Sea (Darmaraki et al., 2019), along the continental shelves of North America (Amaya et al., 2023a) and along the Spanish coast (Fernández-Barba et al., 2024), which concluded that BMHWs tend to last longer than MHWs and that their intensities are often higher than in their surface counterparts. As demonstrated, the Gulf of Trieste BMHW could not have been detected from the surface. A  
395 study of three global ocean reanalysis datasets has shown that this is not uncommon, as about one third of identified subsurface marine heatwaves had no surface signal (Sun et al., 2023). Observational studies of BMHWs (or *sub-surface* MHWs) are rare, since the number of fixed platforms that have been consistently measuring the bottom temperature for more than two decades is rather small. Schaeffer et al. (2023) use a 28-year dataset recorded by a costal mooring located at 53 m isobath off Sydney, Australia. The authors report on three types of marine heatwaves including *sub-surface* marine heatwaves reaching the  
400 bottom. The latter are shown to be caused by downwelling-favorable winds - a different mechanism than in our case, caused by a very different oceanographic setting. Chan et al. (2024) studied MHWs and BMHWs using 20-years of data from five moorings in the Santa Barbara Channel. The sites were even shallower than Vida, with bottom temperatures measured at depths ranging from 9 m to 15 m. About 20% of identified BMHWs in these sites did not have a corresponding MHW signal near the surface. Recent literature (Malan et al., 2025; Capotondi et al., 2024) lists several categories of surface and subsurface marine  
405 heatwaves and the associated driving mechanisms. However, the deepening of the thermocline due to reduced freshwater input is not mentioned as a possible mechanism driving subsurface and bottom heatwaves. It seems this possibility has until now been overlooked, although it may play an important role in areas with reduced precipitation.

The demonstrated lack of surface signal in a significant portion of detected BHWs makes long term bottom measurements of environmental parameters, such as those from Vida, extremely valuable. It also emphasizes the need for more bottom-mounted  
410 thermometers for monitoring, and early warning systems consisting of in situ thermometers in combination with high resolution models such as the MITgcm configuration used in this study.

## 5 Conclusions

The long observational record provided by the Vida buoy allowed us to compare the 2023 bottom temperatures with a long climatological reference and to document one of the rare in situ records of a bottom marine heatwave (BMHW). We show  
415 that the main culprit was an extreme drought that lasted throughout 2022 and into autumn 2023. This preconditioning caused exceptionally high salinity in the surface layers, resulting in weaker water column stratification than usual. Consequently, summer winds that would normally mix only a few meters of the upper water column were able to deepen the mixed layer down to the bottom of the gulf, at  $\sim 20$  m.

Due to the reduced stratification, summer heat was absorbed into a much thicker layer than usual. As a result, surface  
420 overheating was only moderate, while bottom temperatures reached extreme values. This explains why such bottom marine heatwaves cannot be detected from the surface using the usual means, such as satellite-derived sea surface temperature or



surface-mounted thermometers. We also demonstrate that a high-resolution model simulation was able to reproduce the event dynamics and provide a full three-dimensional and temporal evolution of the bottom marine heatwave. Weak stratification was the main driver of the BMHW onset, while subsequent re-stratification due to freshwater inflow trapped heat in the bottom layers and prolonged the event.

In summary, reduced stratification in the GoT caused a deepening of the mixed layer, which in turn led to a BMHW in areas where the bottom usually lies below the mixed layer depth (MLD) but was, in this case, within it. In 2023, this condition applied to a large part of the Gulf of Trieste. This event serves as a warning: regional climate studies (Lionello and Scarascia, 2018; Giorgi and Lionello, 2008) have identified the Mediterranean as a global warming hotspot (Tuel and Eltahir, 2020), where surface marine heatwaves are projected to become increasingly frequent (Konsta et al., 2026; Denamiel, 2025; Galli et al., 2017). One of the projected changes in regional climate, in addition to pronounced warming, is a decrease in total precipitation (Cos et al., 2022). Although recent observational studies have questioned the consistency of past trends implied by these projections (Vicente-Serrano et al., 2025), their potential future realization would further enhance stratification weakening. Under such conditions, the type of preconditioning highlighted here will become more frequent and will likely lead to more frequent, and possibly more intense, BMHWs in the Gulf of Trieste and other similar regions in the Mediterranean Sea and also other shallow stratified areas subjected to droughts worldwide.



*Code and data availability.* Measurements of temperature, salinity and wind at Vida are available at SEANOE: <https://doi.org/10.17882/112596>, Measurements of Isonzo and Rižana runoff are available at ARSO hydrological archive (ARSO, 2025a), Measurements of Po runoff are available at ARPAE (ARPAE, 2025), ERA5 fluxes and precipitation are were obtained from CDS (<https://cds.climate.copernicus.eu/datasets/reanalysis-era5-single-levels?tab=download>). Model outputs (temperature and salinity) subset at the closest grid cell to the Vida buoy are available at <https://doi.org/10.5281/zenodo.18938867>. The model version employed for this study was MITgcm checkpoint68q. Initial and boundary conditions files, as well as runtime namelists and domain bathymetry, for the 5-year run are available at <https://doi.org/10.5281/zenodo.15622740>.

*Author contributions.* FG: modeling and model analysis, conceptualization, writing (original draft preparation), writing (review and editing); ML: conceptualization, writing (original draft preparation), writing (review and editing); SQ: conceptualization, model setup, writing (review and editing); SS: conceptualization, model analysis, writing (review and editing), MV: conceptualization, coordination, writing (original draft preparation), writing (review and editing), in situ data analysis

*Competing interests.* M.L. is a member of the editorial board of Ocean Science.

*Acknowledgements.* M.V. and M.L. acknowledge the financial support from the Slovenian Research Agency (research core funding No. P1-0237). The authors would like to thank Tihomir Makovec for the CTD profiles and Borut Mavrič for encouraging this effort and useful discussions. We thank Elisa Comune and Monica Branchi from ARPAE for their help in obtaining Po discharge data. Special thanks go to Vlado Malačič, Branko Čermelj, Katja Klun and the team who were involved in the design, construction, and maintenance of buoy Vida. We thank Lars Umlauf for the comments on vertical mixing schemes and MLD. This research was funded by the EU Research Infrastructure projects eLTER ERIC.



## 455 References

- Amaya, D. J., Jacox, M. G., Alexander, M. A., Scott, J. D., Deser, C., Capotondi, A., and Phillips, A. S.: Bottom marine heatwaves along the continental shelves of North America, *Nature Communications*, 14, 1038, <https://doi.org/10.1038/s41467-023-36567-0>, 2023a.
- Amaya, D. J., Jacox, M. G., Fewings, M. R., Saba, V. S., Stuecker, M. F., Rykaczewski, R. R., Ross, A. C., Stock, C. A., Capotondi, A., Petrik, C. M., Bograd, S. J., Alexander, M. A., Cheng, W., Hermann, A. J., Kearney, K. A., and Powell, B. S.: Marine heatwaves need  
460 clear definitions so coastal communities can adapt, *Nature*, 616, 29–32, 2023b.
- ARPAE: Dexter, <https://simc.arpae.it/dext3r/>, accessed: 2025-05-19, 2025.
- ARSO: Hydrological Archive, [https://vode.arso.gov.si/hidarhiv/pov\\_arhiv\\_tab.php](https://vode.arso.gov.si/hidarhiv/pov_arhiv_tab.php), accessed: 2025-11-26, 2025a.
- ARSO: Meteorological Archive, <https://meteo.arso.gov.si/met/sl/archive/>, accessed: 2025-05-13, 2025b.
- Azzurro, E., Sbragaglia, V., Cerri, J., Bariche, M., Bolognini, L., Ben Souissi, J., Busoni, G., Coco, S., Chryssanthi, A., Fanelli, E., Ghanem,  
465 R., Garrabou, J., Gianni, F., Grati, F., Kolutari, J., Letterio, G., Lipej, L., Mazzoldi, C., Milone, N., Pannacciulli, F., Pešič, A., Samuel-  
Rhoads, Y., Saponari, L., Tomanic, J., Topçu, N. E., Vargiu, G., and Moschella, P.: Climate change, biological invasions, and the shifting  
distribution of Mediterranean fishes: A large-scale survey based on local ecological knowledge, *Global Change Biology*, 25, 2779–2792,  
<https://doi.org/10.1111/gcb.14670>, 2019.
- Bevilacqua, S., Savonitto, G., Lipizer, M., Mancuso, P., Ciriaco, S., Srijemsi, M., and Falace, A.: Climatic anomalies may create a long-lasting  
470 ecological phase shift by altering the reproduction of a foundation species, *Ecology*, 100, 1–4, 2019.
- Boicourt, W. C., Ličer, M., Li, M., Vodopivec, M., and Malačič, V.: Sea state: Recent progress in the context of climate change, in: *Coastal  
Ecosystems in Transition: A Comparative Analysis of the Northern Adriatic and Chesapeake Bay*, edited by Malone, T. C., Malej, A., and  
Faganeli, J., pp. 21–48, Wiley, <https://doi.org/10.1002/9781119543626.ch3>, 2020.
- Boyd, P. W., Lennartz, S. T., Glover, D. M., and Doney, S. C.: Biological ramifications of climate-change-mediated oceanic multi-stressors,  
475 *Nature Climate Change*, 5, 71–79, <https://doi.org/10.1038/nclimate2441>, 2015.
- Brown, C. J., Mellin, C., Edgar, G. J., Campbell, M. D., and Stuart-Smith, R. D.: Direct and indirect effects of heatwaves on a coral reef  
fishery, *Global Change Biology*, 27, 1214–1225, <https://doi.org/https://doi.org/10.1111/gcb.15472>, 2021.
- Capotondi, A., Rodrigues, R. R., Sen Gupta, A., Benthuisen, J. A., Deser, C., Frölicher, T. L., Lovenduski, N. S., Amaya, D. J., Le Grix,  
N., Xu, T., Hermes, J., Holbrook, N. J., Martinez-Villalobos, C., Masina, S., Koll Roxy, M., Schaeffer, A., Schlegel, R. W., Smith,  
480 K. E., and Wang, C.: A global overview of marine heatwaves in a changing climate, *Communications Earth & Environment*, 5, 701,  
<https://doi.org/10.1038/s43247-024-01806-9>, 2024.
- Carniel, S., Benetazzo, A., Bonaldo, D., Falcieri, F. M., Miglietta, M. M., Ricchi, A., and Sclavo, M.: Scratching beneath the surface while  
coupling atmosphere, ocean and waves: Analysis of a dense water formation event, *Ocean Modelling*, 101, 101–112, 2016.
- Chan, K. Y. K., Kui, L., McDonald, A. M., Ritger, A. L., and Hofmann, G. E.: Coastal marine heatwaves in the Santa Barbara Channel:  
485 decadal trends and ecological implications, *Frontiers in Marine Science*, 11, 1476542, 2024.
- Cos, J., Doblas-Reyes, F., Jury, M., Marcos, R., Bretonnière, P.-A., and Samsó, M.: The Mediterranean climate change hotspot in the CMIP5  
and CMIP6 projections, *Earth System Dynamics*, 13, 321–340, <https://doi.org/10.5194/esd-13-321-2022>, 2022.
- Cosoli, S., Ličer, M., Vodopivec, M., and Malačič, V.: Surface circulation in the Gulf of Trieste (northern Adriatic Sea) from radar, model, and  
ADCP comparisons, *Journal of Geophysical Research: Oceans*, 118, 6183–6200, <https://doi.org/https://doi.org/10.1002/2013JC009261>,  
490 2013.



- Cushman-Roisin, B. and Beckers, J.-M.: Introduction to geophysical fluid dynamics: physical and numerical aspects, vol. 101, Academic press, 2011.
- Darmaraki, S., Somot, S., Sevault, F., and Nabat, P.: Past Variability of Mediterranean Sea Marine Heatwaves, *Geophysical Research Letters*, 46, 9813–9823, <https://doi.org/https://doi.org/10.1029/2019GL082933>, 2019.
- 495 Denamiel, C.: Far-future climate projection of the Adriatic marine heatwaves: a kilometre-scale experiment under extreme warming, *Ocean Science*, 21, 1909–1931, 2025.
- Denaxa, D., Korres, G., Bonino, G., Masina, S., and Hatzaki, M.: The role of air–sea heat flux for marine heatwaves in the Mediterranean Sea, *State of the Planet*, 4, 1–12, 2024.
- Donša, D., Ivajnsič, D., Lipej, L., Trkov, D., Mavrič, B., Pitacco, V., Fortič, A., Lokovšek, A., Šiško, M., and Orlando-Bonaca, M.: Climate-  
500 Driven Habitat Shifts in Brown Algal Forests: Insights from the Adriatic Sea, *Journal of Marine Science and Engineering*, 14, 196, 2026.
- Dulčić, J. and Lipej, L.: The current status of the Adriatic sea fish biodiversity, in: XV European Congress of Ichthyology. *Frontiers Mar. Sci.*, doi: 10.3389/conf.fmars, vol. 73, 2015.
- Escudier, R., Clementi, E., Nigam, T., Aydogdu, A., Fini, E., Pistoia, J., Grandi, A., and Miraglio, P.: Quality Information Document for MED MFC Products "MEDSEA\_MULTIYEAR\_PHY\_006\_004", Tech. rep., Copernicus Marine Service, [https://doi.org/10.25423/](https://doi.org/10.25423/CMCC/MEDSEA_MULTIYEAR_PHY_006_004_E3R1)  
505 [CMCC/MEDSEA\\_MULTIYEAR\\_PHY\\_006\\_004\\_E3R1](https://doi.org/10.25423/CMCC/MEDSEA_MULTIYEAR_PHY_006_004_E3R1), 2024.
- Estournel, C., Estaque, T., Ulses, C., Barral, Q.-B., and Marsaleix, P.: Extreme sensitivity of the northeastern Gulf of Lion (western Mediterranean) to subsurface heatwaves: physical processes and insights into effects on gorgonian populations in the summer of 2022, *Ocean Science*, 21, 1487–1503, <https://doi.org/10.5194/os-21-1487-2025>, 2025.
- Fadeev, E., Hennenfeind, J. H., Amano, C., Zhao, Z., Klun, K., Herndl, G. J., and Tinta, T.: Bacterial degradation of ctenophore *Mnemiopsis*  
510 *leidyi* organic matter, *Msystems*, 9, e01 264–23, 2024.
- Fernández-Barba, M., Huertas, I. E., and Navarro, G.: Assessment of surface and bottom marine heatwaves along the Spanish coast, *Ocean Modelling*, 190, 102 399, 2024.
- Fogarty, M., Ince, L., Hayhoe, K., Mountain, D., and Manning, J.: Potential climate change impacts on Atlantic cod (*Gadus morhua*) off the northeastern USA, *Mitigation and Adaptation Strategies for Global Change*, 13, 453–466, 2008.
- 515 Gačić, M., Lascaratos, A., Manca, B. B., and Mantziafou, A.: Adriatic Deep Water and Interaction with the Eastern Mediterranean Sea, Springer, Dordrecht, [https://doi.org/10.1007/978-94-015-9819-4\\_4](https://doi.org/10.1007/978-94-015-9819-4_4), 2001.
- Galli, G., Solidoro, C., and Lovato, T.: Marine Heat Waves Hazard 3D Maps and the Risk for Low Motility Organisms in a Warming Mediterranean Sea, *Frontiers in Marine Science*, 4, 136, <https://doi.org/10.3389/fmars.2017.00136>, 2017.
- Garrabou, J., Coma, R., Bensoussan, N., Bally, M., Chevaldonné, P., Cigliano, M., Díaz, D., Harmelin, J.-G., Gambi, M. C., Kersting, D. K.,  
520 Ledoux, J. B., Lejeusne, C., Linares, C., Marschal, C., Pérez, T., Ribes, M., Romano, J.-C., Serrano, E., Teixidó, N., Torrents, O., Zabala, M., Zuberer, F., and Cerrano, C.: Mass mortality in Northwestern Mediterranean rocky benthic communities: effects of the 2003 heat wave, *Global Change Biology*, 15, 1090–1103, <https://doi.org/10.1111/j.1365-2486.2008.01823.x>, 2009.
- Garrabou, J., Gómez-Gras, D., Medrano, A., Cerrano, C., Ponti, M., Schlegel, R., Bensoussan, N., Turicchia, E., Sini, M., Gerovasileiou, V., Teixidó, N., Mirasole, A., Tamburello, L., Cebrian, E., Rilov, G., Ledoux, J.-B., Ben Souissi, J., Khamassi, F., Ghanem, R., Ben-  
525 abdi, M., Grimes, S., Ocaña, O., Bazairi, H., Hereu, B., Linares, C., Kersting, D. K., Rovira, G., Ortega, J., Casals, D., Pagès-Escolà, M., Margarit, N., Capdevila, P., Verdura, J., Ramos, A., Izquierdo, A., Barbera, C., Rubio-Portillo, E., Anton, I., López-Sendino, P., Díaz, D., Vázquez-Luis, M., Duarte, C. M., Marbà, N., Aspillaga, E., Espinosa, F., Grech, D., Guala, I., Azzurro, E., Farina, S., Gambi, M. C., Chimienti, G., Montefalcone, M., Azzola, A., Mantas, T. P., Frascchetti, S., Ceccherelli, G., Kipson, S., Bakran-Petricioli, T.,



- Petricioli, D., Jimenez, C., Katsanevakis, S., Kizilkaya, I. T., Kizilkaya, Z., Sartoretto, S., Ruitton, S., Comeau, S., Gattuso, J.-P., and Harmelin, J.-G.: Marine heatwaves drive recurrent mass mortalities in the Mediterranean Sea, *Global Change Biology*, 28, 5708–5725, <https://doi.org/10.1111/gcb.16301>, 2022.
- Gaspar, P., Grégoris, Y., and Lefevre, J.: A simple eddy kinetic energy model for simulations of the oceanic vertical mixing: Tests at station Papa and long-term upper ocean study site, *Journal of Geophysical Research: Oceans*, 95, 16 179–16 193, <https://doi.org/10.1029/JC095iC09p16179>, 1990.
- 535 Gianni, F., Falace, A., Orlando-Bonaca, M., Ciriaco, S., Ivajnsič, D., Kaleb, S., Lipej, L., Mavrič, B., Querin, S., and Bandelj, V.: Environmental alterations and sea warming drive seagrass meadow decline in urbanized coastal areas of the northern Adriatic Sea, *Estuarine, Coastal and Shelf Science*, p. 109563, 2025.
- Gill, A. E.: *Atmosphere—ocean dynamics*, Academic Press, 1982.
- Giordano, F. and Querin, S.: Initial and boundary conditions and namelists for the MITgcm northern Adriatic Sea 2017-2021 hindcasts, <https://doi.org/10.5281/zenodo.15622740>, 2025.
- 540 Giorgi, F. and Lionello, P.: Climate change projections for the Mediterranean region, *Global and Planetary Change*, 63, 90–104, <https://doi.org/https://doi.org/10.1016/j.gloplacha.2007.09.005>, mediterranean climate: trends, variability and change, 2008.
- Glamuzina, B., Vilizzi, L., Piria, M., Žuljević, A., Cetinić, A. B., Pešić, A., Dragičević, B., Lipej, L., Pećarević, M., Bartulović, V., et al.: Global warming scenarios for the Eastern Adriatic Sea indicate a higher risk of invasiveness of non-native marine organisms relative to current climate conditions, *Marine Life Science & Technology*, 6, 143–154, 2024.
- 545 Gómez-Gras, D., Linares, C., López-Sanz, À., Amate, R., Ledoux, J.-B., Bensoussan, N., Drap, P., Bianchimani, O., Marschal, C., Torrents, O., Zuberer, F., Cebrian, E., Teixidó, N., Zabala, M., Kipson, S., Kersting, D. K., Montero-Serra, I., Pagès-Escolà, M., Medrano, A., Milani, A., Frleta-Valić, M., Dimarchopoulou, D., López-Sendino, P. C., and Garrabou, J.: Population collapse of habitat-forming species in the Mediterranean: A long-term study of gorgonian populations affected by recurrent marine heatwaves, *Proceedings of the Royal Society B: Biological Sciences*, 288, 20212 384, <https://doi.org/10.1098/rspb.2021.2384>, 2021.
- 550 Grisogono, B. and Belušić, D.: A review of recent advances in understanding the meso- and microscale properties of the severe Bora wind, *Tellus A*, 61, 1–16, <https://doi.org/https://doi.org/10.1111/j.1600-0870.2008.00369.x>, 2009.
- Gruber, N., Boyd, P. W., Frölicher, T. L., and Vogt, M.: Biogeochemical extremes and compound events in the ocean, *Nature*, 600, 395–407, <https://doi.org/10.1038/s41586-021-03981-7>, 2021.
- 555 Gómez-Gras, D., Linares, C., Dornelas, M., Madin, J. S., Brambilla, V., Ledoux, J.-B., López-Sendino, P., Bensoussan, N., and Garrabou, J.: Climate change transforms the functional identity of Mediterranean coralligenous assemblages, *Ecology Letters*, 24, 1038–1051, <https://doi.org/https://doi.org/10.1111/ele.13718>, 2021.
- Hamdeno, M. and Alvera-Azcaráte, A.: Marine heatwaves characteristics in the Mediterranean Sea: Case study the 2019 heatwave events, *Frontiers in Marine Science*, 10, 1093 760, <https://doi.org/10.3389/FMARS.2023.1093760>, 2023.
- 560 Hersbach, H., Bell, B., Berrisford, P., Hirahara, S., Horányi, A., Muñoz-Sabater, J., Nicolas, J., Peubey, C., Radu, R., Schepers, D., Simons, A., Soci, C., Abdalla, S., Abellan, X., Balsamo, G., Bechtold, P., Biavati, G., Bidlot, J., Bonavita, M., De Chiara, G., Dahlgren, P., Dee, D., Diamantakis, M., Dragani, R., Flemming, J., Forbes, R., Fuentes, M., Geer, A., Haimberger, L., Healy, S., Hogan, R. J., Hólm, E., Janisková, M., Keeley, S., Laloyaux, P., Lopez, P., Lupu, C., Radnoti, G., de Rosnay, P., Rozum, I., Vamborg, F., Villaume, S., and Thépaut, J.-N.: The ERA5 Global Reanalysis, *Quarterly Journal of the Royal Meteorological Society*, 146, 1999–2049, <https://doi.org/10.1002/qj.3803>, 2020.
- 565



- Hobday, A. J., Alexander, L. V., Perkins, S. E., Smale, D. A., Straub, S. C., Oliver, E. C., Benthuisen, J. A., Burrows, M. T., Donat, M. G., Feng, M., Holbrook, N. J., Moore, P. J., Scannell, H. A., Sen Gupta, A., and Wernberg, T.: A hierarchical approach to defining marine heatwaves, *Progress in Oceanography*, 141, 227–238, <https://doi.org/10.1016/j.pocean.2015.12.014>, 2016.
- Hobday, A. J., Oliver, E. C., Gupta, A. S., Benthuisen, J. A., Burrows, M. T., Donat, M. G., Holbrook, N. J., Moore, P. J., Thomsen, M. S., Wernberg, T., and Smale, D. A.: Categorizing and naming marine heatwaves, *Oceanography*, 31, 162–173, 2018.
- Holbrook, N. J., Scannell, H. A., Sen Gupta, A., Benthuisen, J. A., Feng, M., Oliver, E. C. J., Alexander, L. V., Burrows, M. T., Donat, M. G., Hobday, A. J., Moore, P. J., Perkins-Kirkpatrick, S. E., Smale, D. A., Straub, S. C., and Wernberg, T.: A global assessment of marine heatwaves and their drivers, *Nature Communications*, 10, 1–13, <https://doi.org/10.1038/s41467-019-10206-z>, 2019.
- Kara, A. B., Rochford, P. A., and Hurlburt, H. E.: An optimal definition for ocean mixed layer depth, *Journal of Geophysical Research: Oceans*, 105, 16 803–16 821, <https://doi.org/10.1029/2000JC900072>, 2000.
- Konsta, K., Katsanevakis, S., Stranga, Y., and Mazaris, A. D.: Increasing bottom marine heatwaves pose a critical risk to Mediterranean benthic species, *Cell Reports Sustainability*, 2026.
- Large, W. G., McWilliams, J. C., and Doney, S. C.: Oceanic vertical mixing: A review and a model with a nonlocal boundary layer parameterization, *Reviews of Geophysics*, 32, 363–403, <https://doi.org/10.1029/94RG01872>, 1994.
- Ličer, M., Smerkol, P., Fettich, A., Ravdas, M., Papapostolou, A., Mantziafou, A., Strajnar, B., Cedilnik, J., Jeromel, M., Jerman, J., Petan, S., Malačič, V., and Sofianos, S.: Modeling the ocean and atmosphere during an extreme bora event in northern Adriatic using one-way and two-way atmosphere–ocean coupling, *Ocean Science*, 12, 71–86, 2016.
- Lionello, P. and Scarascia, L.: The relation between climate change in the Mediterranean region and global warming, *Regional Environmental Change*, 18, <https://doi.org/10.1007/s10113-018-1290-1>, 2018.
- Lipej, L. and Moskon, S.: ON THE RECORD OF THE MORAY EEL (*MURAENA HELENA* LINNAEUS, 1758) IN SLOVENIAN COASTAL WATERS (GULF OF TRIESTE, NORTHERN ADRIATIC)/PRIMA SEGNALAZIONE DI MURENA MEDITERRANEA (*MURAENA HELENA* LINNAEUS, 1758) IN ACQUE COSTIERE SLOVENE (GOLFO DI TRIESTE, ADRIATICO SETTENTRIONALE), in: *Annales: Series Historia Naturalis*, vol. 21, p. 157, Scientific and Research Center of the Republic of Slovenia, 2011.
- Lipej, L. and Rogelja, M.: Status of the invasive blue crab *Callinectes sapidus* Rathbun, 1896 (Brachyura: Portunidae) in Slovenia, *Acta Biologica Slovenica*, 64, 24–33, 2021.
- Lombardo, D., Flora, S., Giordano, F., Ingrassia, E., Menna, M., Querin, S., and Ursella, L.: Influence of wind stress and the Isonzo/Soča River outflow on surface currents in the Gulf of Trieste, *EGUsphere*, 2025, 1–30, <https://doi.org/10.5194/egusphere-2025-1176>, 2025.
- Malačič, V.: Wind direction measurements on Moored coastal buoys, *Journal of Atmospheric and Oceanic Technology*, 36, 1401–1418, 2019.
- Malačič, V., Šonc, D., and Petelin, B.: Coastal oceanographic station at the entrance of the Gulf of Trieste (Northern Adriatic), in: *Elsevier Oceanography Series*, vol. 69, pp. 361–365, Elsevier, 2003.
- Malačič, V., Celio, M., Čermelj, B., Bussani, A., and Comici, C.: Interannual evolution of seasonal thermohaline properties in the Gulf of Trieste (NA) 1991–2003, *Journal of Geophysical Research: Oceans*, 111, <https://doi.org/10.1029/2005JC003267>, 2006.
- Malan, N., Sen Gupta, A., Schaeffer, A., Zhang, S., Doblin, M. A., Semolini Pilo, G., Kiss, A. E., Everett, J. D., Behrens, E., Capotondi, A., Cravatte, S., Hobday, A. J., Holbrook, N. J., Kajtar, J. B., and Spillman, C. M.: Lifting the lid on Marine Heatwaves, *Progress in Oceanography*, p. 103539, <https://doi.org/10.1016/j.pocean.2025.103539>, 2025.
- Malej, A., Tirelli, V., Lučić, D., Paliaga, P., Vodopivec, M., Goruppi, A., Ancona, S., Benzi, M., Bettoso, N., Camatti, E., Ercolessi, M., Ferrari, C. R., and Shiganova, T.: *Mnemiopsis leidyi* in the northern Adriatic: here to stay?, *Journal of Sea Research*, 124, 10–16, <https://doi.org/10.1016/j.seares.2016.12.005>, 2017.



- Marshall, J. and Schott, F.: Open-ocean convection: Observations, theory, and models, *Reviews of geophysics*, 37, 1–64, 1999.
- 605 Marshall, J., Adcroft, A., Hill, C., Perelman, L., and Heisey, C.: A finite-volume, incompressible Navier Stokes model for studies of the ocean on parallel computers, *Journal of Geophysical Research: Oceans*, 102, 5753–5766, <https://doi.org/https://doi.org/10.1029/96JC02775>, 1997.
- Martellucci, R., Paladini de Mendoza, F., Menna, M., Pirro, A., Reale, M., Gačić, M., Poulain, P.-M., Riminucci, F., Le Meur, J., Giordano, P., Langone, L., Cardin, V., Cantoni, C., Bergami, C., Grilli, F., Marini, M., Gallo, A., Notarstefano, G., Toller, S., Bastianini, M., Krali, M., Diociaiuti, T., Pacciaroni, M., Bussani, A., Miserocchi, S., and Mauri, E.: A multiobservation analysis of the 2017 dense water formation events: Climate change, bottom density currents, and Adriatic-Ionian sea circulation (Mediterranean Sea), *Journal of Geophysical Research: Oceans*, 130, e2024JC022306, <https://doi.org/10.1029/2024JC022306>, 2025.
- 610 Mavrič, B., Ivajnsič, D., Lučić, D., Malej, A., and Lipej, L.: Feeding Habits of the Invasive Ctenophore *Mnemiopsis leidyi* in the Gulf of Trieste (Adriatic Sea), *Water*, 17, 470, 2025a.
- 615 Mavrič, B., Schliewen, U., Heß, M., Hervat, M., and Melzer, R.: First record for the Gulf of Venice: Mediterranean Cardinal fish, *Apogon imberbis* (Linnaeus, 1758), spotted in the Brijuni Marine Protected Area and marine caves at the slopes of Banjol Island (Croatia)(Teleostei, Apogonidae), *Spixiana*, 47, 259–260, 2025b.
- Mihanović, H., Vilibić, I., Carniel, S., Tudor, M., Russo, A., Bergamasco, A., Bubić, N., Ljubešić, Z., Viličić, D., Boldrin, A., Malačić, V., Celio, M., Comici, C., and Fabio, R.: Exceptional dense water formation on the Adriatic shelf in the winter of 2012, *Ocean science*, 9, 561–572, 2013.
- 620 Mihanović, H., Janeković, I., Vilibić, I., Kovačević, V., and Bensi, M.: Modelling interannual changes in dense water formation on the northern Adriatic shelf, in: *Meteorology and Climatology of the Mediterranean and Black Seas*, pp. 345–361, Springer, 2019.
- Pastor, F. and Khodayar, S.: Marine heat waves: Characterizing a major climate impact in the Mediterranean, *Science of The Total Environment*, 861, 160 621, <https://doi.org/10.1016/j.scitotenv.2022.160621>, 2023.
- 625 Pastor, F., Paredes-Fortuny, L., and Khodayar, S.: Mediterranean marine heatwaves intensify in the presence of concurrent atmospheric heatwaves, *Communications Earth & Environment*, 5, 797, <https://doi.org/10.1038/s43247-024-01982-8>, 2024.
- Pisano, A., Fanelli, C., Ciani, D., Tronconi, C., Cesarini, C., La Padula, F., and Buongiorno Nardelli, B.: Mediterranean Sea High Resolution and Ultra High Resolution Sea Surface Temperature Analysis SST\_MED\_SST\_L4\_NRT\_OBSERVATIONS\_010\_004, Tech. rep., Copernicus Marine Service, <https://doi.org/https://doi.org/10.48670/moi-00172>, 2024.
- 630 Plecha, S. M. and Soares, P. M.: Global marine heatwave events using the new CMIP6 multi-model ensemble: from shortcomings in present climate to future projections, *Environmental Research Letters*, 15, 124 058, 2020.
- Poulain, P.-M. and Cushman-Roisin, B.: *Circulation*, pp. 67–109, Springer Netherlands, Dordrecht, [https://doi.org/10.1007/978-94-015-9819-4\\_3](https://doi.org/10.1007/978-94-015-9819-4_3), 2001.
- Poulain, P.-M. and Raicich, F.: *Forcings*, pp. 45–65, Springer Netherlands, Dordrecht, [https://doi.org/10.1007/978-94-015-9819-4\\_2](https://doi.org/10.1007/978-94-015-9819-4_2), 2001.
- 635 Price, J. F.: On the scaling of stress-driven entrainment experiments, *Journal of Fluid Mechanics*, 90, 509–529, 1979.
- Querin, S., Cossarini, G., and Solidoro, C.: Simulating the formation and fate of dense water in a midlatitude marginal sea during normal and warm winter conditions, *Journal of Geophysical Research: Oceans*, 118, 885–900, 2013.
- Querin, S., Bensi, M., Cardin, V., Solidoro, C., Bacer, S., Mariotti, L., Stel, F., and Malačić, V.: Saw-tooth modulation of the deep-water thermohaline properties in the southern Adriatic Sea, *Journal of Geophysical Research: Oceans*, 121, 4585–4600, 2016.



- 640 Querin, S., Cosoli, S., Gerin, R., Laurent, C., Malačič, V., Pristov, N., and Poulain, P.-M.: Multi-Platform, High-Resolution Study of a Complex Coastal System: The TOSCA Experiment in the Gulf of Trieste, *Journal of Marine Science and Engineering*, 9, <https://doi.org/10.3390/jmse9050469>, 2021.
- Rečnik, K., Klun, K., Lipej, L., Malej, A., and Tinta, T.: Chemical composition and egg production capacity throughout bloom development of ctenophore *Mnemiopsis leidyi* in the northern Adriatic Sea, *PeerJ*, 12, e17 844, 2024.
- 645 Rivetti, I., Frascchetti, S., Lionello, P., Zambianchi, E., and Boero, F.: Global warming and mass mortalities of benthic invertebrates in the Mediterranean Sea, *PloS one*, 9, e115 655, 2014.
- Rodrigues, R. R., Artana, C., Gonçalves Neto, A., Frölicher, T. L., Keenlyside, N., Hobday, A. J., Burger, F. A., Bernardo, P. S., and Araújo, J.: Extreme compound events in the equatorial and South Atlantic, *Nature Communications*, 16, 3183, <https://doi.org/10.1038/s41467-025-58238-y>, 2025.
- 650 Russo, A., Carniel, S., Sclavo, M., and Krzjelj, M.: Climatology of the Northern-Central Adriatic Sea, in: *Modern Climatology*, edited by Wang, S.-Y. S. and Gillies, R. R., chap. 7, IntechOpen, Rijeka, <https://doi.org/10.5772/34693>, 2012.
- Schaeffer, A., Sen Gupta, A., and Roughan, M.: Seasonal stratification and complex local dynamics control the sub-surface structure of marine heatwaves in Eastern Australian coastal waters, *Communications Earth & Environment*, 4, 304, 2023.
- Simon, A., Plecha, S. M., Russo, A., Teles-Machado, A., Donat, M. G., Auger, P.-A., and Trigo, R. M.: Hot and cold marine extreme events  
655 in the Mediterranean over the period 1982–2021, *Frontiers in Marine Science*, 9, 892 201, 2022.
- Smale, D. A., Wernberg, T., Oliver, E. C. J., Thomsen, M., Harvey, B. P., Straub, S. C., Burrows, M. T., Alexander, L. V., Benthuisen, J. A., Donat, M. G., Feng, M., Hobday, A. J., Holbrook, N. J., Perkins-Kirkpatrick, S. E., Scannell, H. A., Sen Gupta, A., Payne, B. L., and Moore, P. J.: Marine heatwaves threaten global biodiversity and the provision of ecosystem services, *Nature Climate Change*, 9, 306–312, <https://doi.org/10.1038/s41558-019-0412-1>, 2019.
- 660 Smith, K. E., Burrows, M. T., Hobday, A. J., King, N. G., Moore, P. J., Sen Gupta, A., Thomsen, M. S., Wernberg, T., and Smale, D. A.: Biological impacts of marine heatwaves, *Annual review of marine science*, 15, 119–145, 2023.
- Sun, D., Li, F., Jing, Z., Hu, S., and Zhang, B.: Frequent marine heatwaves hidden below the surface of the global ocean, *Nature Geoscience*, 16, 1099–1104, 2023.
- Tuel, A. and Eltahir, E. A.: Why is the Mediterranean a climate change hot spot?, *Journal of Climate*, 33, 5829–5843, 2020.
- 665 Umlauf, L. and Burchard, H.: Second-order turbulence closure models for geophysical boundary layers. A review of recent work, *Continental Shelf Research*, 25, 795–827, 2005.
- Vicente-Serrano, S. M., Tramblay, Y., Reig, F., González-Hidalgo, J. C., Beguería, S., Brunetti, M., Kalin, K. C., Patalen, L., Kržič, A., Lionello, P., Lima, M. M., Trigo, R. M., El-Kenawy, A. M., Eddenjal, A., Türkes, M., Koutroulis, A., Manara, V., Maugeri, M., Badi, W., Mathbout, S., Bertalanič, R., Bocheva, L., Dabanli, I., Dumitrescu, A., Dubuisson, B., Sahabi-Abed, S., Abdulla, F., Fayad, A., Hodzic, S.,  
670 Ivanov, M., Radevski, I., Peña-Angulo, D., Lorenzo-Lacruz, J., Domínguez-Castro, F., Gimeno-Sotelo, L., García-Herrera, R., Franquesa, M., Halifa-Marín, A., Adell-Michavila, M., Noguera, I., Barriopedro, D., Garrido-Perez, J. M., Azorin-Molina, C., Andres-Martin, M., Gimeno, L., Nieto, R., Llasat, M. C., Markonis, Y., Selmi, R., Ben Rached, S., Radovanović, S., Soubeyroux, J.-M., Ribes, A., Saidi, M. E., Bataineh, S., El Khalki, E. M., Robaa, S., Boucetta, A., Alsafadi, K., Mamassis, N., Mohammed, S., Fernández-Duque, B., Cheval, S., Moutia, S., Stevkov, A., Stevkova, S., Luna, M. Y., and Potopová, V.: High temporal variability not trend dominates Mediterranean  
675 precipitation, *Nature*, 639, 658–666, <https://doi.org/10.1038/s41586-024-08576-6>, 2025.
- Vodopivec, M., Zaimi, K., and Peliz, Á. J.: The freshwater balance of the Adriatic Sea: a sensitivity study, *Journal of Geophysical Research: Oceans*, 127, e2022JC018 870, 2022.

<https://doi.org/10.5194/egusphere-2026-2567>

Preprint. Discussion started: 13 May 2026

© Author(s) 2026. CC BY 4.0 License.



Vodopivec, M., Malačič, V., Čermelj, B., and Klun, K.: Vida buoy temperature, salinity and wind measurements, <https://doi.org/10.17882/112596>, 2026.

680 von Schuckmann, K., Moreira, L., Cancet, M., Gues, F., Autret, E., Baker, J., Bricaud, C., Bourdalle-Badie, R., Castrillo, L., Cheng, L., et al.: The state of the global ocean, *State of the Planet*, 4, 1–30, 2024.

WMO: WMO Guidelines on the Calculation of Climate Normals, Tech. Rep. WMO-No. 1203, World Meteorological Organization, Geneva, Switzerland, 2017.